THE UNIVERSITY OF CALGARY

ARCH ACTION in DEEP CONCRETE SANDWICH BEAMS AND SLABS

BY

M. W. SMYTH

A THESIS

SUBMITTED TO THE FACULTY OF GRADUATE STUDIES

IN PARTIAL FULFILLMENT OF THE REQUIREMENTS FOR THE DEGREE OF MSc

DEPARTMENT OF CIVIL ENGINEERING

CALGARY, ALBERTA

FEBRUARY, 1990

ISBN 0-315-61759-4

THE UNIVERSITY OF CALGARY

FACULTY OF GRADUATE STUDIES

The undersigned certify that they have read, and recommend to the Faculty of Graduate Studies for acceptance, a thesis entitled, "Arch Action in Deep Concrete Sandwich Beams and Slabs", submitted by M. W. Smyth in partial fulfillment of the requirements for the degree of Master of Science.

A. Ghali

Chairman, Dr. A. Ghali
Department of Civil Engineering

R Loov

Dr. R. E. Loov
Department of Civil Engineering

Mansa Singh

Dr. M. C. Singh
Department of Mechanical Engineering

Tariq Nasseri

Dr. T. Nasseri
Centre for Frontier Engineering Research

Date FEBRUARY 21, 1990

Abstract

In any deep beam or slab, a part of the out of plane load is supported by bending action, and part is carried by Arching, or Compressive Membrane Action (CMA). This work is an investigation of CMA in sandwich type deep beams and slabs comprised of two steel plates on the exterior surfaces with concrete between. A parametric study utilizing the non-linear finite element program FELARC (Finite Element Layered Analysis of Reinforced Concrete) of a concrete beam with a span to depth ratio of 4, loaded with a concentrated load at mid-span is conducted. The parameters varied, in order of importance, include span to depth ratio, in-plane stiffness at the support, amount and location of longitudinal steel, and type of shear connection between the steel and concrete.

An increase in the span to depth ratio was found to result in a proportional decrease in the load carried by CMA. The in-plane stiffness at the support was varied from a small value to infinitely stiff, resulting in increased ultimate load capacity. An increase in the amount of longitudinal reinforcing steel both top and bottom was found to result in only a small increase in the ultimate load capacity.

An analytical model developed for the simple case of a rigidly restrained, unreinforced concrete beam is shown to give comparable results to the finite element model, both for ultimate load capacity and deflection.

A three dimensional finite element model of a one way slab with three one meter spans, a thickness of 0.25 m, and steel plates amounting to 2.6% reinforcement both top and bottom, is analyzed for a concentrated load at the middle of the centre span. Comparison of principal compression stress vector plots from the non-linear

three dimensional case with the corresponding non-linear two dimensional case show that the load carrying mechanism and stress distributions are substantially different. In the two dimensional case, load can only be transferred directly to the support, however in the three dimensional case load is transferred perpendicular to the supports, resulting in what is essentially two way arching, ie. a dome effect.

The use of two dimensional models to study three dimensional effects is of marginal benefit because these load carrying mechanisms are sufficiently different as to render any comparison questionable. However, because the mechanisms are of the same type, it is expected that the relative importance of the factors considered in the two dimensional study would be the same in the three dimensional case.

It is concluded that when testing physical specimens or conducting numerical analysis of deep beams and slabs, it is of utmost importance to properly model the support conditions and load application details. In particular, improper modelling of the in-plane restraint at the free edges of the specimen could cause a serious underestimation of the load carrying capacity and ductility of such members. When designing deep beams and slabs, consideration of the beneficial effects of CMA could result in considerable cost savings.

Recommendations are made regarding the development of a three dimensional non-linear finite element program. A very stable solution technique and concrete model with the capability of modelling tension stiffening and the descending portion of the compression side of the stress-strain curve should be implemented, as should an interface element for bond slip modelling. A post processing program capable of selective printing and plotting of results is considered mandatory in order to allow analysis of the results.

Acknowledgements

Thanks and gratitude are owed to a great many people, but none more than Dr. Amin Ghali, whose guidance was invaluable. He was at all times fair and flexible, and who can ask more from any man. The wisdom imparted by Dr. Robert Loov during several fruitful discussions kept the author on track at an important stage of the work. Dr. Walter Dilger was the first person to explain compressive membrane action in terms simple enough for the author to comprehend.

The financial support granted by Dr. Peter Adams and the Centre for Frontier Engineering Research (CFER), without which this work would not have been possible, is gratefully acknowledged. In addition, the financial support of the Canadian Society for Civil Engineering/Donald Jamieson Scholarship committee, who honoured the author as the first recipient of this award, is also gratefully acknowledged.

Tom Zimmerman of CFER provided much useful information, and the benefit of his experience in conducting many tests of sandwich beams and slabs. Every consultant at Academic Computer Services provided the author with immediate solutions to seemingly unsolvable problems, and saved a great deal of time.

Finally, my wife Cindy provided inspiration and motivation when it seemed that the end was nowhere in sight.

What saved the Doric temple from structural collapse was that the stone beams were short and deep and, as they cracked, they turned themselves into arches.

J. E. Gordon, Structures (or Why Things Don't Fall Down)

Contents

List of Tables

List of Figures

Notation

a	depth of concrete strut
b	depth of beam
DOF	degree of freedom
E_{CS}	secant stiffness of concrete at maximum compressive stress
E_0	tangent stiffness of concrete at zero strain
E_S	elastic modulus of steel
E_S^*	strain hardening modulus of steel
f_y	yield strength of steel
f'_c	uniaxial compressive strength of concrete
H	horizontal reaction
l	length of beam
l_1	original length of compression strut
l_2	deformed length of compression strut
Mn	minimum stress
Mx	maximum stress
P	applied point load
u_i	translational DOF at node i
v_i	translational DOF at node i
w	width of beam
x, y, z	cartesian coordinate system
y_1	original height of compression strut

y_2	deformed height of compression strut
α	ratio of σ_1/σ_2
β	cracked shear retention factor
β	angle of rotation of compression strut
δ	deflection
Δl	change in length of compression strut
Δy	vertical deflection of strut
ε	strain
ε_{cu}	concrete strain at maximum compressive stress
ε_t	maximum elastic tensile concrete strain
ε_{tu}	ultimate concrete strain in tension
ε_u	ultimate strain at failure
θ	angle between the undeformed strut and horizontal
θ_i	rotational DOF at node i
σ	stress
σ_x	stress in x direction
σ_y	stress in y direction
σ_1, σ_2	principal stress

Chapter 1

Introduction

1.1 General

The work presented herein is a parametric study of compressive membrane, or arching, action in deep beams and slabs using the finite element method. Parameters under consideration include the amount of in-plane restraint, amount of reinforcing steel both top and bottom, amount and type of shear reinforcing steel, and the span to depth ratio. The finite element method has been used exclusively, no physical specimens were tested.

Two nonlinear finite element programs were used in this study. FELARC (Finite Element Analysis of Reinforced Concrete) developed by G. A. M. Ghoneim at the University of Calgary was used to conduct a parametric study of a two dimensional concrete beam. This program was modified to allow it to interface with a specially developed plotting program in order to allow direct plotting of deformed shapes, crack orientations, principal compressive stresses, and material states.

The other program used in this work was ANSYS, a powerful commercial finite element package developed by Swanson Analysis Systems. This program is available for academic use at the University of Calgary, and was used to conduct a study of a three dimensional concrete slab.

Compressive membrane action (CMA) has been recognized and understood, at least qualitatively, almost since reinforced concrete was first utilized. However, CMA is generally ignored in design because of difficulties in analysis, and because certain parameters are difficult to quantify, vary a great deal from case to case, and have a great effect on the load carrying capacity. By far the most important is the restraint provided by neighbouring beams or slabs in a continuous system. The amount of longitudinal (in the case of a beam) or in-plane (in the case of a slab) restraint provided by members in adjacent bays depends upon the loading conditions, the span to depth ratio, the presence or absence of cracks, and the support conditions, in addition to many other factors.

The situation is summed up very well by Cope and Clark (1984), who state:

> "Despite considerable research effort, the analytical solutions developed were too complicated for use in design and depend on parameters that are difficult to quantify in actual slab systems. ... In general, therefore, compressive membrane enhancement is not explicitly taken into account by codes of practice for building slabs. ... As the results of more realistic analyses and large scale tests become available, it is likely that future design practice will take more note of the effects of membrane enhancement.

In fact the current bridge design code in the province of Ontario (1979) allows for CMA in the design of reinforced concrete bridge decks. A substantial reduction in the amount of transverse reinforcing steel is the result of consideration of the beneficial effects of CMA.

The present study has been partially funded by the Centre for Frontier Engineering Research (CFER) who are investigating the behaviour of deep (span to depth ratios of four to six) steel-concrete panels in which the concrete is sandwiched between two exterior steel plates. These panels, as illustrated in Figure 1.1 (after Maddock and Bruce, 1984), have recently been proposed for use in Arctic Offshore applications, mainly as exterior members of bottom founded exploration and production platforms for the oil industry. In this application, the panels would be subjected to very high intensity out of plane ice forces. Another possible application is in the protection of military targets from missile attack.

Sandwich construction techniques are used in many applications where high strength and/or stiffness in combination with lightness are required. Examples abound in everyday life:

- doors made of plywood and paper
- corrugated cardboard
- sailboats made of fiberglass on balsa
- the Space Shuttle is fabricated of sandwiched aluminum panels

The anticipated advantages of steel and concrete panels include:

- good resistance to local indentation and buckling
- high load capacity
- excellent resistance to brittle failure at low temperatures and high loading rates
- excellent ductility with little reduction in load capacity
- no excess weight of concrete cover over the steel

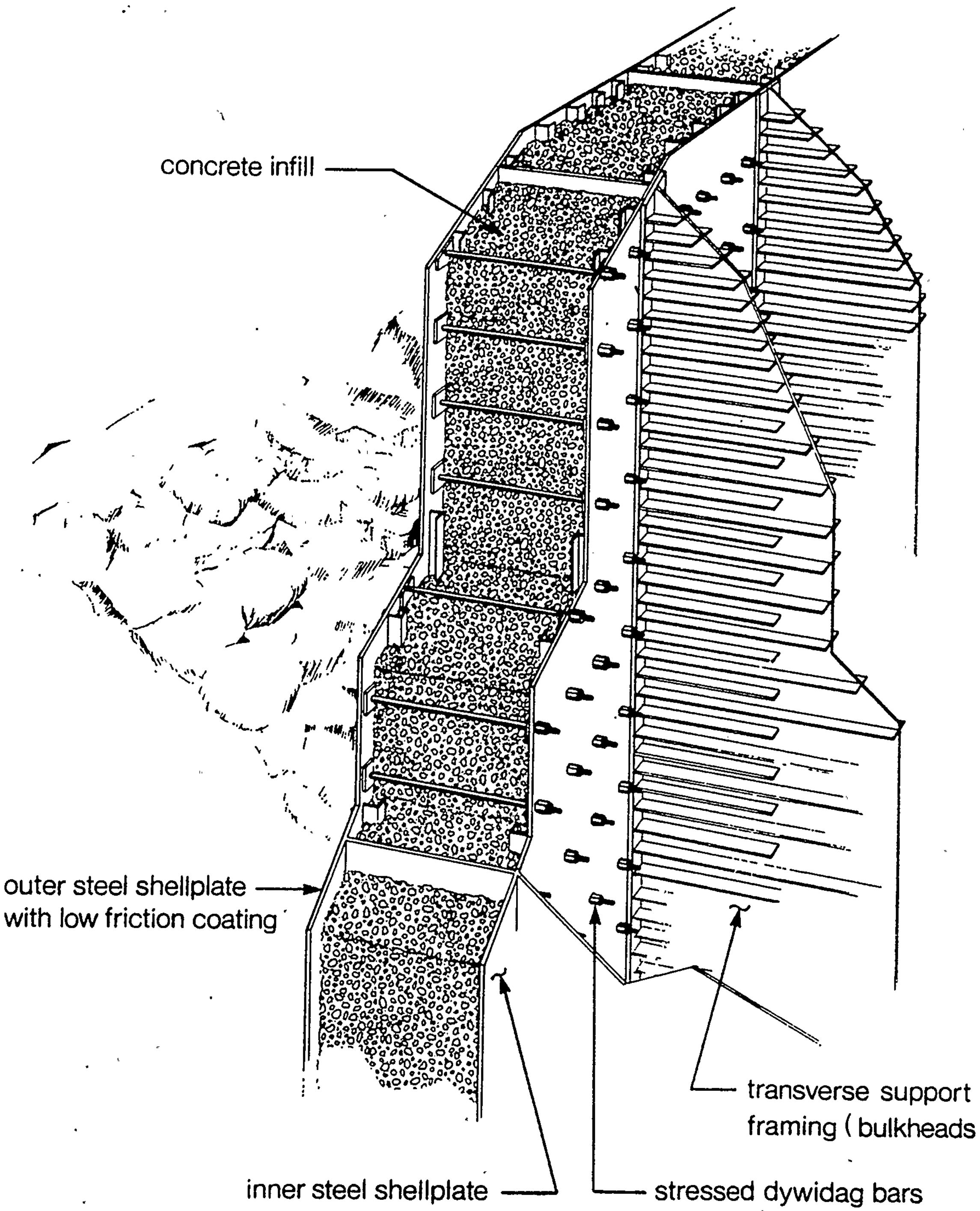

Figure 1.1: Steel - Concrete Composite Ice Wall

- the steel provides a self supporting formwork for ease of construction
- allows rapid construction in conventional facilities

Other groups of researchers around the world are investigating this method of construction, however to date there has yet to be a major structure fabricated in this manner. Dome Petroleum's very successful Single Steel Drilling Caison (SSDC), a bottom founded arctic drilling platform designed and built in 1982, has sandwich type exterior ice resisting walls made of concrete and steel. However, the concrete is simply a load spreading medium to the load resisting steel beams and bulkheads behind. The design did not rely on composite action at all, and therefore CMA was not considered.

1.2 Compressive Membrane Action

Compressive membrane action is a term usually used to refer to a three dimensional structure, for example a slab. Arching action is usually used to refer to a two dimensional member such as a beam, however the two effects are essentially the same. For the sake of simplicity both will be collectively referred to as Compressive Membrane Action (CMA) in this work.

CMA is a phenomenon whereby out of plane loads are resisted primarily by in-plane compressive stresses rather than by bending and shear stresses. It is somewhat analogous to tensile membrane action, but with a subtle difference. Tensile membrane action can occur for any ductile material provided suitable support conditions exist. However, CMA can only occur if the material has a tensile strength lower than its compressive strength, such as concrete. It is because of this dependance

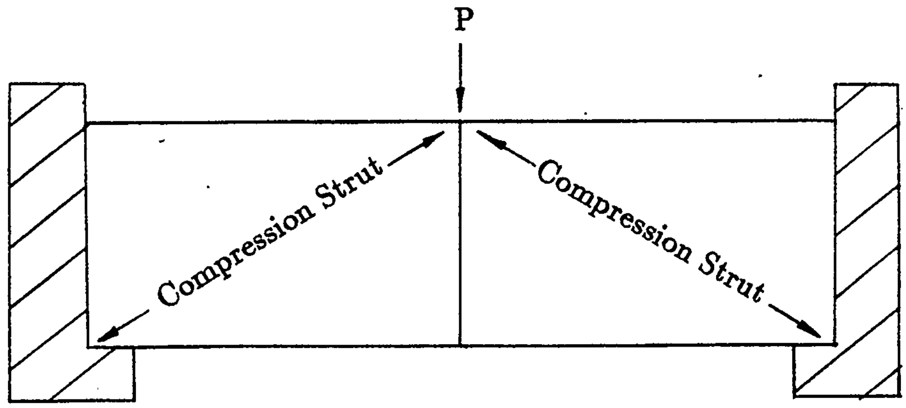

Figure 1.2: Simplified Model of Compressive Membrane Action

upon non-linear behaviour that a linear-elastic beam analysis, or even a deep beam analysis, will not provide proper results where CMA is involved.

The simplest way to visualize compressive membrane action is to imagine two bricks wedged between two immovable walls as shown in Figure 1.2. A load applied to the bricks will be resisted by compressive forces only as indicated. As long as the compressive stress does not exceed the crushing strength of the material, the structure will resist load and will not collapse.

This simplified discussion can be applied to concrete beams as well. Suppose that, instead of two bricks, we have an unreinforced concrete beam wedged between immovable supports as shown in Figure 1.3. As load is applied to the concrete beam, a tensile crack will develop in the bottom of the member below the load and the beam will separate from the supports at the top of the member. This situation is analogous to a tied arch. If the immovable support is replaced by an infinitely stiff unbonded reinforcing rod as shown in Figure 1.4, the net result will be the same. Therefore it

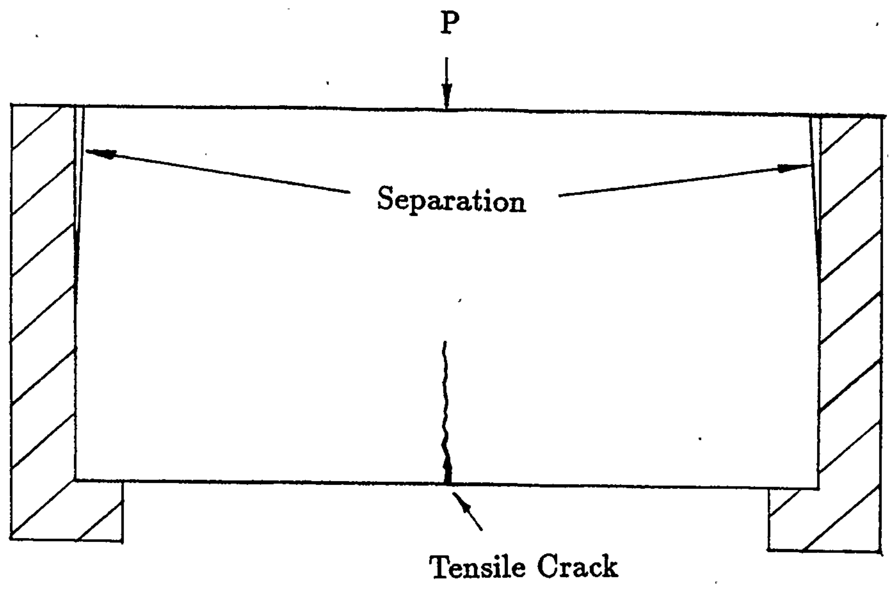

Figure 1.3: Wedged Concrete Beam

can be seen that the effect of in-plane restraint at the ends of the beam is similar to longitudinal reinforcing steel in the bottom of the member.

In reality an immovable support is impossible to obtain, but several situations provide sufficient fixity to allow CMA to develop. For example, a continuous concrete beam with similar loading in each span as shown in Figure 1.5 will behave almost as if it had immovable supports at each reaction point. Because of symmetry, a vertical line above each support will neither rotate or translate, and therefore each span can be considered to have immovable supports. CMA will be present, cracks will develop in the locations indicated on Figure 1.5, and the ultimate strength of the beam will be limited by the compressive strength of the concrete. Any steel provided in the member will be more or less redundant. Steel would possibly alter the compression field in the concrete but would not appreciably alter the compression membrane load of the member. It is possible that the steel could develop tensile membrane action, and if there were enough steel in the beam, the load carried in tensile membrane

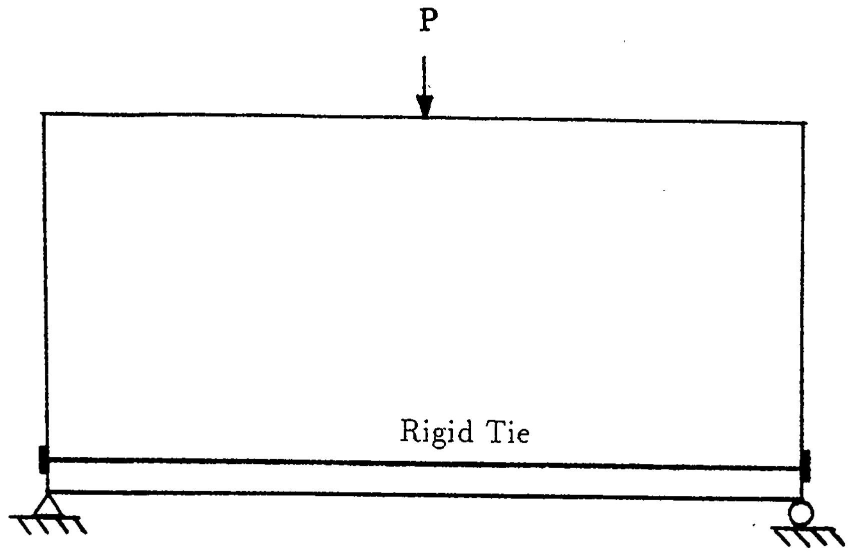

Figure 1.4: Concrete Beam with Unbonded Reinforcing Rod

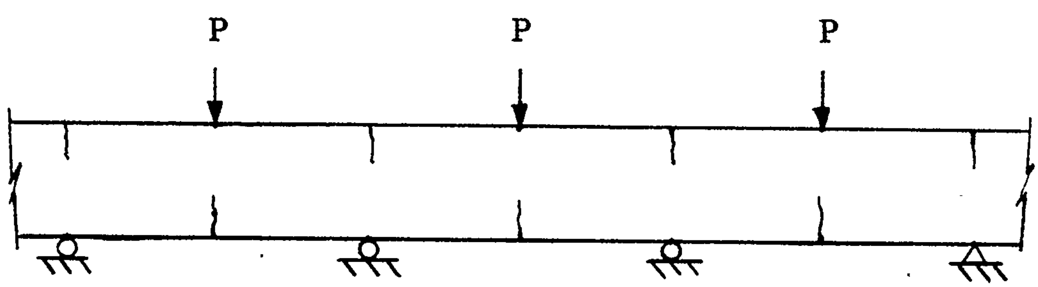

Figure 1.5: Continuous Concrete Beam

action could exceed that of CMA.

Similarly, a continuous concrete beam with only one span loaded will also develop CMA. Because symmetry of loading is not present in this case, there would be some translation and rotation of the support. The supports could no longer be considered as immovable, but would have some finite stiffness. Depending upon the actual amount of in-plane restraint provided by the continuous beam, a considerable amount of load may be carried by CMA.

It is very easy to extend these concepts into three dimensions and consider a slab instead of a beam. If a slab is partially or completely restrained against in-plane movement on its boundary, for example by neighbouring slabs or beams, then CMA will develop. Once again, the amount of load that can be carried will depend upon the amount of in-plane restraint provided at the boundary of the slab.

Chapter 2

Literature Review

2.1 Introduction

Two subject areas will be covered in this literature review. The first is compressive membrane action (CMA), and the second is sandwich beams and slabs. In conducting this literature review, it was discovered that there has been virtually no overlap of the two subjects. That is, investigators studying CMA have not considered sandwich panels, and vice versa. This is not surprising because, for the most part investigators in the area of CMA have dealt with conventional bridge decks and building slabs. On the other hand, work in the area of sandwich panels is fairly recent, and has concentrated mainly on understanding the behaviour of these panels in general terms, in particular on understanding the influence of various types of shear connectors. However, the majority of research into CMA has direct application to sandwich beams and slabs.

2.2 Compressive Membrane Action

An excellent historical review of work done in this area is provided by Braestrup (1980), and the following is a brief summary.

The early pioneers of reinforced concrete understood the concepts of CMA as illustrated in texts by Westergaard and Slater (1921) and Taylor, Thompson and

Smulski (1925). CMA was relied upon even by early design codes, which allowed slabs to be designed which contained less longitudinal reinforcing steel than would be required by a simple bending calculation, using the given loads, safety factors, and material properties. The codes indirectly recognized that some load carrying mechanism, other than bending, was contributing to the resistance of the member. After World War Two, most experimental investigations were designed to test the validity of yield line theory. Consequently, all possible care was taken to prevent the occurrence of membrane forces. Ockleston (1955) provided the impetus for a resurgence in research in this area when he reported on tests conducted on floor slabs of a three storey reinforced concrete building. He recorded collapse loads of three to four times the capacities predicted by yield line theory, and identified the cause as compressive membrane action.

The American Concrete Institute (ACI) annual convention in 1971 addressed the questions of cracking, deflection, and ultimate load of concrete slab systems. The papers presented at this conference, as well as several others, were published in ACI publication SP-30. Some of these papers are reviewed here.

Brotchie and Holley (1971) conducted an extensive series of tests on 45 square slabs. Parameters varied included span to depth ratio, reinforcement ratio, and the boundary support conditions. In summary they found:

- An increase in the in-plane restraint at the boundary increased both the load capacity and the stiffness of the slab.
- For unreinforced specimens with in-plane restraint, the increase in capacity is proportional to the thickness cubed.

- The increase in capacity with increasing reinforcement ratio is less marked. For example, with a span to depth ratio of five, the increase in capacity provided by 3.0% reinforcing steel is only 50% above the unreinforced case.

- For a span to depth ratio of five, the capacity of the unreinforced restrained slab is 1.8 times that of the simply supported case with 3.0% reinforcing steel on the bottom.

- For thin slabs it is essential to provide full edge restraint in order to develop membrane action. However, for thicker slabs some displacement at the edges may be tolerated without significantly reducing the load capacity.

- For a span to depth ratio of five, the loading intensity is of the same order of magnitude as the induced flexural stress. The effect of normal stress on the load capacity is significant. The plastic deformability of concrete in a triaxial state is large.

The authors did not account for creep in their experiment, but anticipate that it will have most influence on thin slabs, and lesser influence on thick slabs.

Hopkins and Park (1971) report the results of a quarter scale, nine panel reinforced concrete slab and beam floor designed with an allowance for membrane action. They point out that the entire slab must be designed as a unit, rather than taking each panel as a separate entity. The slab contained about 0.15% reinforcing steel in each of the two orthogonal directions in both the top and the bottom surfaces. The span to depth ratio of the centre panel was 32, and that of the edge panels was 23. The slab was supported at the intersection points of the beams.

The entire surface of the slab was designed to carry 800 pounds per square foot. As designed, the expected ratio of ultimate load to yield line theory load was 2.0 for the centre panel, 1.35 for the centre edge panels, and 1.0 for the corner panels. The actual measured ratios at failure were 2.18, 1.55, and 1.46 respectively. The authors concluded that design allowing for membrane action is possible, but that in practice the applicability will be limited to relatively thick, heavily loaded slabs with reliable in-plane restraint.

Tong and Batchelor (1971) reported results of tests conducted on scale models of bridge decks with a span to depth ratio of 25. Point loads representing wheel loads were applied. It was found that CMA enhanced both the flexural and the shear capacity of the deck. If the steel reinforcement ratio was low, a flexural type failure resulted. If a higher reinforcement ratio was used, a punching shear type failure resulted. For each model the longitudinal and transverse reinforcement ratios were the same.

In a continuation of the above work, Hewitt and Batchelor (1975) describe a rational approach for calculating the punching strength of slabs with known boundary restraints. They adopted and enhanced a failure model originally proposed by Kinnunen and Nylander (1960). After verifying the applicability of the model to simply supported slabs by comparing actual and predicted punching strength values for 165 tests, they go on to compare results of several slabs with in-plane restraint. In both cases excellent agreement was obtained.

In the process of analyzing the slabs with in-plane restraint, the authors show that considering a continuous slab as an equivalent slab simply supported at the line of contraflexure considerably underestimates the punching shear capacity of the slab.

The reason for this is that the beneficial effects of CMA are ignored.

The results of Hewitt and Bachelor's work have been incorporated into the Ontario Bridge Code (1979), resulting in a substantial reduction of the transverse reinforcing steel required in deck slabs of bridges designed and built in that province.

Kirkpatrick, Rankin and Long (1984) report results of twenty one-third scale tests on M-beam type bridge deck slabs. This type of bridge deck is standard in the United Kingdom, and essentially consists of precast, pretensioned, concrete beams supporting a cast in place reinforced concrete deck. The beam spacing was varied from 1.5 to 2.0 m, and the transverse reinforcement ratio was varied from 0.25% to 1.7%. The load was a simulated wheel load. The authors found that all panels, regardless of the reinforcement ratio, failed at about the same load. They go on to propose an equation for the ultimate shear force capacity based on a modified punching shear equation. Enhancement due to compressive membrane action is accounted for by an equivalent reinforcement parameter, and the actual transverse reinforcement ratio is neglected.

Kirkpatrick, Rankin and Long (1986) furthered the above mentioned work by conducting full scale serviceability tests on a 160 mm thick reinforced concrete bridge deck of an M-beam type bridge. The beam spacing and reinforcement ratios were varied as they were in the previous tests.

The authors concluded that initial cracking is independent of bar size and is mainly dependent on concrete strength. At service load all test panels were uncracked. If the slab is overloaded and cracked, and subsequently reloaded to 1 and to 3.5 times the service load, the resulting cracks are 7 to 10 times smaller than those predicted by the current British Code (BS 5400). It is suggested that 12 mm diameter bars at 150 mm spacing are more than adequate for both ultimate and service load behaviour for 160 mm thick slabs with beams spaced at up to 2.0 m.

2.3 Sandwich Construction

In a series of four reports prepared in the late 1970's, Matsuishi et. al. describe a comprehensive set of tests conducted on composite steel and concrete sandwich beams.

The first of these reports (Matsuishi et. al., 1977) describes tests conducted to establish the ultimate strength of sandwich beams with various shear connection details. Each beam had a span of 2.25 m, depth of 0.4 m, and width of 0.3 m, resulting in a span to depth ratio of 5.6. Transverse diaphragms connected the top and bottom plates at the quarter points, and the beam was loaded at the centre line with a single point load. The simply supported beams had no in-plane end restraint whatsoever. The shear connectors examined included angles welded to the top and bottom plates transverse to the length of the beam, flat bar stiffeners welded to the top and bottom plates in the longitudinal direction and headless shear studs made from reinforcing steel welded perpendicular to both plates. The authors concluded that:

- Conventional reinforced concrete analysis agrees well with the results.
- The manner of shear connection had little influence on the ultimate strength.
- The depth of the section and the area of the tension steel are the most significant factors with respect to the ultimate strength.

- Deformation before failure is very large and the structure can absorb a great deal of energy before failure.

In the second paper (Matsuishi et. al., 1978) the authors performed a non-linear finite element analysis using constant strain triangle elements. The effects of cracking, plastification of both steel and concrete, and slip between the steel and concrete were included. Excellent agreement with the test results of the first paper were obtained.

In the third report (Matsuishi et. al., 1980) the effect of repeated loading was examined. It was concluded that, other than the possibility of developing a fatigue crack at the fillet weld joining the tension plate and the diaphragm, repeated loading did not have any effect on the behaviour of the members.

Finally, the effect of a longitudinal diaphragm was examined (Matsuishi et. al., 1980). The addition of a single longitudinal diaphragm, which essentially converted the member into a steel "I" beam with concrete at the sides, increased the ultimate capacity of the member by 100%. The amount of the increase was almost equal to the shear capacity of the added web, indicating that the member strength was still governed by it's capacity in shear.

A special subsection of POAC (Port and Ocean Engineering under Arctic Conditions) 87 addressed the issue of composite steel and concrete sandwich construction in offshore applications. Several informative papers were presented.

Matsuishi and Iwata (1987) tested four types of members with various arrangements of shear connectors loaded with both point loads and uniformly distributed load. In one series of tests "T" stiffeners running longitudinally were compared to

"T" stiffeners running transversely. It was found that the longitudinal arrangement increased the ultimate load carrying capacity by 53% for a point load and by 23% for a uniformly distributed load in comparison to the transversely oriented stiffeners.

Several two span continuous beams were subjected to various freeze/thaw cycles prior to testing to failure. It was found that freeze/thaw had no effect on the ultimate strength performance of the member.

Zimmerman, MacGregor, and Adams (1987) report the results of two sandwich beams tested under a uniformly distributed load. Each beam had a depth of 250 mm, a width of 275 mm, and a span between the centre line of the supports of 1000 mm. The bearing surface at the supports was 150 mm long, and the beam had an overhanging cantilever portion of 237 mm. Transverse diaphragms were provided at the quarter points. No other shear connection between the steel and concrete was provided. The only difference between the two specimens was in the details of the supports providing the reaction to the beam. In the first case steel rollers were used which eliminated any possibility of any horizontal reaction at the support. In the second case a teflon pad was used which provided a horizontal force of about 3% of the normal force.

In the first case the member failed in bending, specifically the tension plate fractured, at a load of 8.2 MPa. In the second case, the member failed in shear at a load of 9.5 MPa. However, it did not collapse at this load. The test continued on and the load reduced to 7.5 MPa, and then gradually increased back to 9.5 MPa again. At this point the test was stopped because the deformation exceeded the limits of the load frame. The deflection in the second case was more than double that of the first case. This illustrates the sensitivity of beams of this type to the actual support conditions.

The authors go on to show that the bending moment capacity is accurately predicted using conventional reinforced concrete truss analysis. However, the shear capacity is more difficult to predict. An empirical approach based on Zsutty (1968) is shown to produce good agreement with the results, as does an upper bound plasticity approach based on work by Nielsen and Braestrup (1978, 1984).

O'Flynn and MacGregor (1987) report the results of seventeen beam type sandwich specimens loaded with a uniformly distributed load. The physical dimensions are similar to the specimens tested by Zimmerman and others, except the span varies from 1.0 m to 1.5 m. Stud shear connectors attached to both top and bottom plates are used to provide the shear connection between the steel and concrete rather than the transverse diaphragms as Zimmerman used. Ultimate strengths were virtually the same as those reported by Zimmerman. A third method of calculating shear force capacity based on a lower bound plasticity theory is shown to compare well with test results.

Smith and McLeish (1987) report the results of tests conducted on a sandwich shell which had a constant radius of curvature in one direction of 1829 mm. The span of the shell was 2286 mm and the depth of the section was about 150 mm. A 2 mm steel plate was provided top and bottom. Shear connection was provided with transverse diaphragms spaced at approximately 75 mm. The behaviour of this shell was compared to that of an ordinary reinforced concrete shell which had similar geometry and arrangement of reinforcing, but had three times as much flexural steel. The load deflection curves are not appreciably different, except that the sandwich shell carried 19% more load than the conventional slab. The reason for the similar behaviour in spite of the substantial difference in the amount of flexural steel is that the sandwich panel maximizes the lever arm between the two steel layers, whereas a conventional reinforced concrete shell has a large amount of concrete cover which reduces the effectiveness of the steel in bending.

In addition to testing a sandwich shell, two flat slabs were also tested, each with a span of 2.8 m. "L" shaped stiffeners almost as deep as the section alternately connected to the top and bottom plates provided the shear connection. In one panel these connectors were arranged transversely and in the other they were arranged longitudinally. Testing showed that the slab with the longitudinal arrangement was roughly 30% stiffer and carried 30% more load. Both tests were stopped prior to collapse for safety reasons.

2.4 Summary

The following points are particularly relevant to this study and bear repeating.

- Hopkins and Park (1971) showed that when designing for CMA, the entire slab must be designed as a unit, rather than designing each individual panel in isolation. This is mainly because the boundary conditions at the panel interfaces are difficult to model.

- Kirkpatrick, Rankin and Long showed that, in addition to benefiting the ultimate load carrying capacity, CMA also improves serviceability requirements.

- The Ontario Bridge Code (1979), based on work done by Hewitt and Batchelor (1975) and others, incorporated CMA into the design requirements for the transverse reinforcement of concrete bridge decks, substantially reducing the amount of steel required.

- In the past ten years, most researchers investigating the behaviour of sandwich panels have concentrated on the method of shear connection between the steel and concrete. The evidence seems to indicate that the method of shear connection is not critical to the performance of the members tested. No researcher has investigated the effects of CMA in sandwich panels.

- Zimmerman's (1987) tests of two deep sandwich beams vividly illustrate the importance of in-plane restraint at the boundary on the behaviour of these types of members. The addition of a horizontal force at the support amounting to only 3% of the vertical reaction changed the mode of failure from bending to shear, increased the ultimate load in excess of 15%, and increased the ductility in excess of 100%.

Chapter 3

Two Dimensional Parametric Study

3.1 Introduction

Results of a parametric study conducted with the non-linear finite element program FELARC (Finite Element Layered Analysis of Reinforced Concrete) (1978) are presented. The study focuses on the behaviour of a deep concrete beam loaded with a single point load at the centre. The beam measures 1.0 m long, 0.25 m deep, and 0.375 m wide, resulting in a span to depth ratio of four. The main parameters varied include the in-plane restraint at the support, the amount and location of longitudinal steel, the amount and type of shear connection steel, and the span to depth ratio, which was varied by increasing the length of the beam.

Initial investigations indicated that a mesh of 24 in-plane elements, 6 along the half length and 4 through the depth, would provide sufficient accuracy. Symmetry of the beam is used to advantage so that only half the beam is actually modelled. Gaussian numerical integration of order 2x2 is used to evaluate the material properties and to formulate the stiffness matrix for each element.

The program FELARC was modified to store the results for each load step, thus allowing post-processing and plotting of the results at a later date. The following information can be plotted using the post processing program:

- Deformed mesh geometry

- Principal compression stress at each Gauss point
- Material states at each Gauss point
- Load deflection curves for any node and degree of freedom.

The program Tel-A-Graf was used to perform the actual plotting. This program is a front end processor for the DISSPLA plotting subroutines, and is available for use on the Honeywell Multics system at the University of Calgary.

3.2 Theoretical Compression Strut Model

A simplified analytical model of an unreinforced beam is presented. The analysis is similar to those of Braestrup (1980) and Brotchie and Holley (1971) who each used a rigid-plastic formulation for the same problem. The current formulation is based on a linear elastic analysis and uses the equivalent rectangular stress block commonly used in the design of reinforced concrete members.

Consider a concrete beam which is completely restrained against in-plane motion at each end, and which has no reinforcing steel as shown in Figure 3.1a. A load P is applied at the centre of the beam. It is assumed that the concrete beam will crack on the bottom surface at the beam centre line and will separate from the supports on the top surface. The end result is that the load will be supported by two struts of depth a. This situation is represented by the force diagram shown in Figure 3.1b.

From simple statics we can write equation 3.1.

$$P = 4H(b-a)/l \tag{3.1}$$

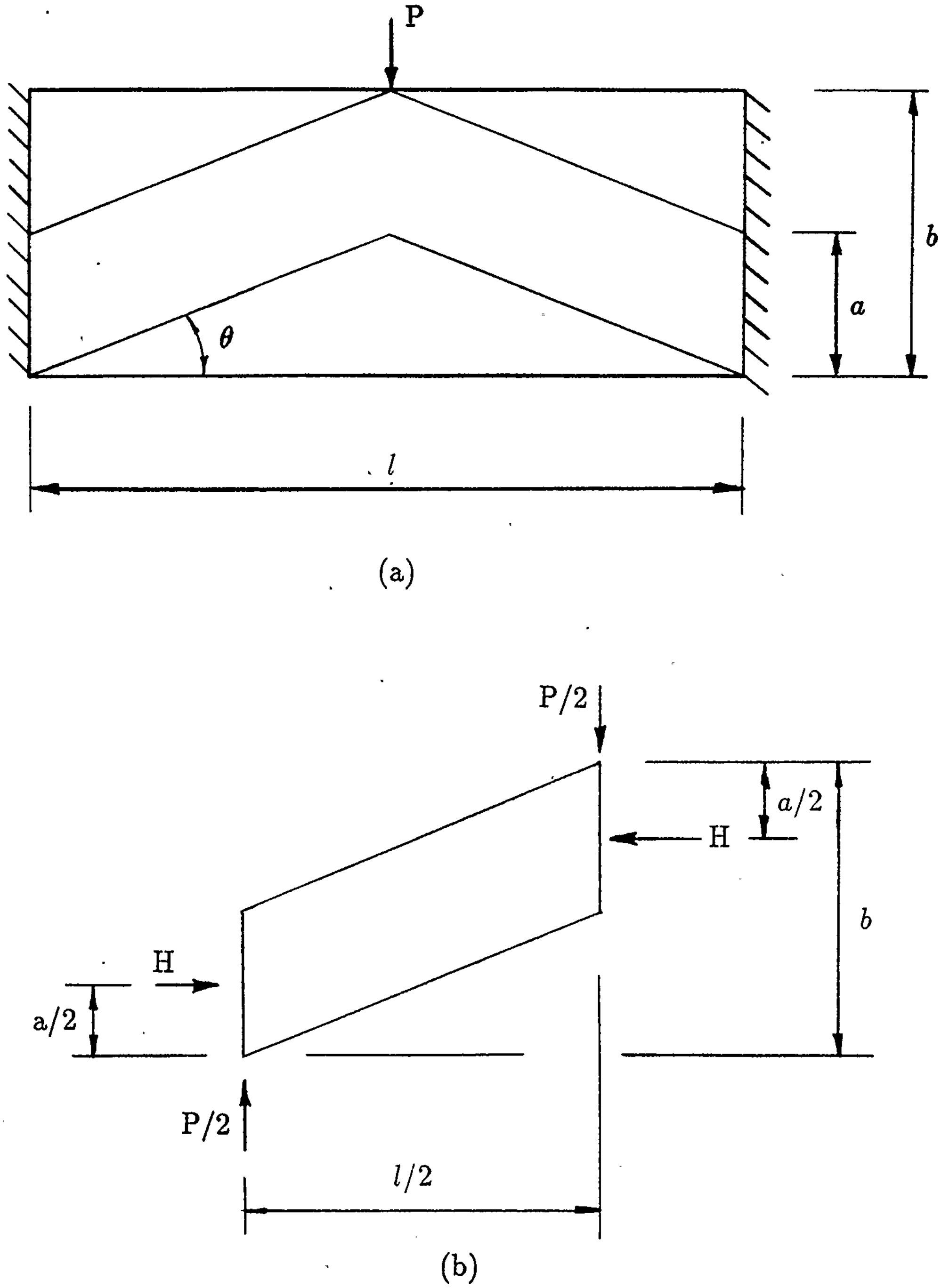

Figure 3.1: Beam With Ends Restrained In-Plane

Using the equivalent rectangular stress block, the force H may be calculated using equation 3.2, where w is the width of the beam.

$$H = .85 f'_c a w \tag{3.2}$$

Subsituting equation 3.2 into 3.1 leads to equation 3.3, which may be used to calculate P, the force that the beam can support

$$P = 0.85 \times 4 f'_c w a(b - a)/l \tag{3.3}$$

In order to maximize the value of P, equation 3.3 is differentiated with respect to a and equated to zero, resulting in equation 3.4. From this equation we obtain $a = b/2$ for maximum P.

$$0.85 \times 4 f'_c w(b - 2a)/l = 0 \tag{3.4}$$

From this equation we obtain $a = b/2$ for maximum P. The maximum value of P is calculated using equation 3.5.

$$P_{max} = 0.85 f'_c w b^2/l \tag{3.5}$$

In order to calculate the deflection of the beam due to P_{max}, consider the strut shown in Figure 3.2. If the assumption is made that the angle the strut rotates through when the load is applied, β, is small in comparison to the original angle of the strut, θ (this is valid for deep beams only), then equation 3.6 applies.

$$\Delta y \approx \Delta l \times l_1/y_1 \tag{3.6}$$

Futhermore, assume the maximum compression occurs in the strut at a strain of ε_{cu}, therefore Δl may be calulated using equation 3.7

$$\Delta l = \varepsilon_{cu} l_1 \tag{3.7}$$

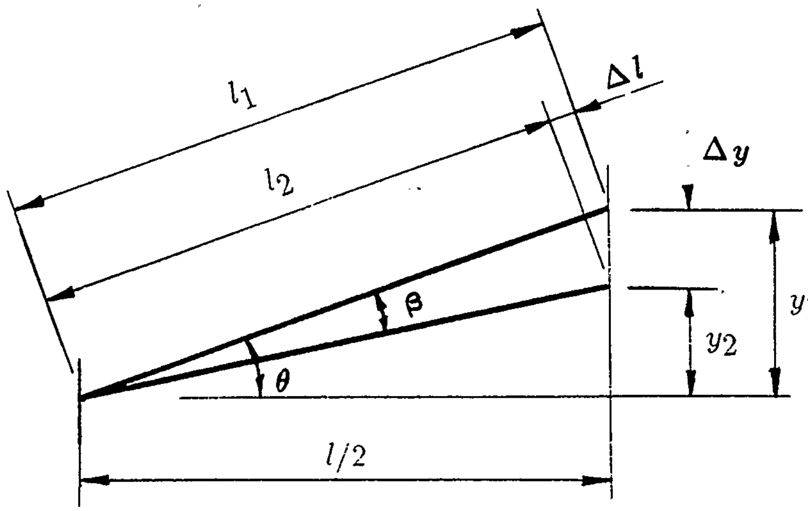

Figure 3.2: Geometry of Deflected Strut

Substituting equation 3.7 into 3.6 leads to equation 3.8.

$$\Delta y = \varepsilon_{cu} l_1^2 / y_1 \tag{3.8}$$

From Pythagorus we can write equation 3.9.

$$l_1^2 = y_1^2 + (l/2)^2 \tag{3.9}$$

Substituting equation 3.9 into 3.8, we obtain equation 3.10.

$$\Delta y = \varepsilon_{cu}(y_1^2 + (l/2)^2)/y_1 \tag{3.10}$$

Now, assuming the maximum compression in the strut occurs at a strain of 0.002, and substituting $y_1 = b/2$, we obtain equation 3.11, which may be used to calculate the deflection of the beam at P_{max} in most cases.

$$\Delta y = 0.002 \left[\left(\frac{b}{2}\right)^2 + \left(\frac{l}{2}\right)^2 \right] \frac{2}{b} \tag{3.11}$$

If the beam is not deep enough (ie. a span to depth ratio less than 10) to allow the assumption of small angles of deflection, then the deflection may be calculated more accurately using equation 3.12.

$$\Delta y = y_1 - \left[y_1^2 - 0.004 \times (l^2/4 + y_1^2) \right]^{0.5} \tag{3.12}$$

For a beam with a span to depth ratio of 5, the error between equation 3.12 and the approximate deflection is 2.6%.

The deflection calculated with either equation 3.11 or 3.12 will be larger than the actual deflection for two reasons. First, the strut will actually be thicker than what has been assumed for most of its length, resulting in smaller stresses and strains than assumed. The second influence is the presence of tension in the concrete, which will contribute somewhat to the load carrying capacity of the beam, making it slightly more stiff.

3.3 The Finite Element Program FELARC

FELARC (Finite Element Layered Analysis of Reinforced Concrete) is a non-linear finite element program developed at the University of Calgary by Ghoneim (1978). A users manual written by Ghoneim and Ghali (1979) explains all that is necessary to use the program. FELARC is intended for the analysis of reinforced concrete and is non-linear in the sense that material non-linearities are considered, however geometric non-linearities are not. The effects of prestressing, cyclic loading, creep, shrinkage, and temperature stress are considered. The element library includes:

- a shell element formulated by combining a rectangular bending element with an in-plane element

- a truss element
- a boundary element used to calculate reaction forces and to represent non-rigid supports

With these features FELARC is a useful tool for analyzing concrete beams, shear panels, slabs, folded plates, shells, and box girders.

FELARC uses an incremental iterative tangent stiffness solution procedure in which the stiffness matrix is updated at each iteration of each increment. The tangential stiffness matrix calculated at the end of each iteration is used to estimate deflections in the subsequent iteration. The program allows a force norm or a displacement norm to be used in determining the convergence and divergence at any particular iteration. Unbalanced forces at each node at the end of each iteration are calculated by relying on the fact that there is a unique, albeit non-linear, relationship between stress and strain.

3.3.1 Material Models

Figure 3.3 (after Ghoneim, 1978) presents the uniaxial stress-strain curve adopted for use in FELARC. The compressive loading curve up to the point of maximum loading is based on equation 3.13 first suggested by Saenz (1968).

$$\sigma = \frac{E_0 \varepsilon}{1 + [E_0/E_{cs} - 2]\,\varepsilon/\varepsilon_{cu} + [\varepsilon/\varepsilon_{cu}]^2} \tag{3.13}$$

The descending part of the compressive stress-strain curve is based on equation 3.14, proposed by Smith and Young (1955).

$$\sigma = f'_c \left[\frac{\varepsilon}{\varepsilon_{cu}}\right] e^{[1 - \varepsilon/\varepsilon_{cu}]} \tag{3.14}$$

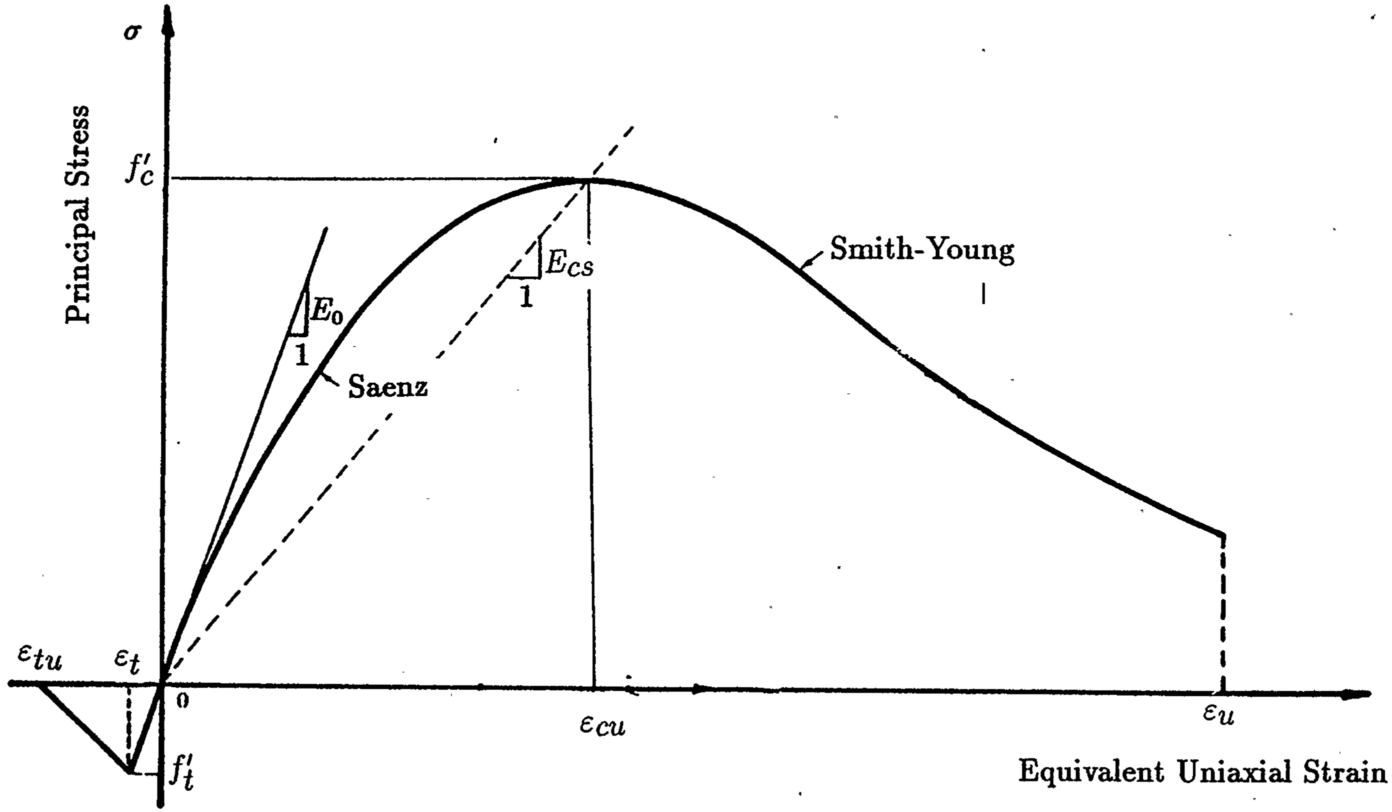

Figure 3.3: Equivalent Uniaxial Stress-Strain Relationship

On the tension side, cracking is assumed to start when the principal stress exceeds the uniaxial tensile strength f_t' of the concrete. In order to better model the actual behaviour of the reinforced concrete, and to provide a more stable solution procedure, tension stiffening is incorporated into the program. This means that instead of unloading immediately upon exceeding the the tensile strength of the concrete, the unloading occurs gradually. In fact, the program uses a discontinuous step function to unload the tensile forces in order to avoid numerical difficulties associated with negative stiffness.

Biaxial states of stress are accounted for using the biaxial failure envelope illustrated in Figure 3.4 (after Ghoneim, 1978). Values of f_c' on the uniaxial stress strain curve (Figure 3.3) are determined from this failure envelope developed by Kupfer and Gerstle (1973).

FELARC adopts a bilinear material model for the behaviour of reinforcing steel as illustrated in Figure 3.5. The behaviour is fully defined by four constants, namely, yield strength (f_y), elastic modulus (E_s), strain hardening modulus (E_s^*), and ultimate strain (ε_u).

3.3.2 The QLC3 Finite Element

The program employs the element QLC3 (an acronym for Quadrilateral, Linear Cubic, Three degrees of freedom) derived by Sisodiya (1971) to perform in plane analysis. The element was developed for the economic analysis of in plane loading when beam-like behaviour dominates. The element has three degrees of freedom at each node, displacement in the x and y directions, and rotation about the out of plane direction. As expected, it performs very well when used to model beams, webs

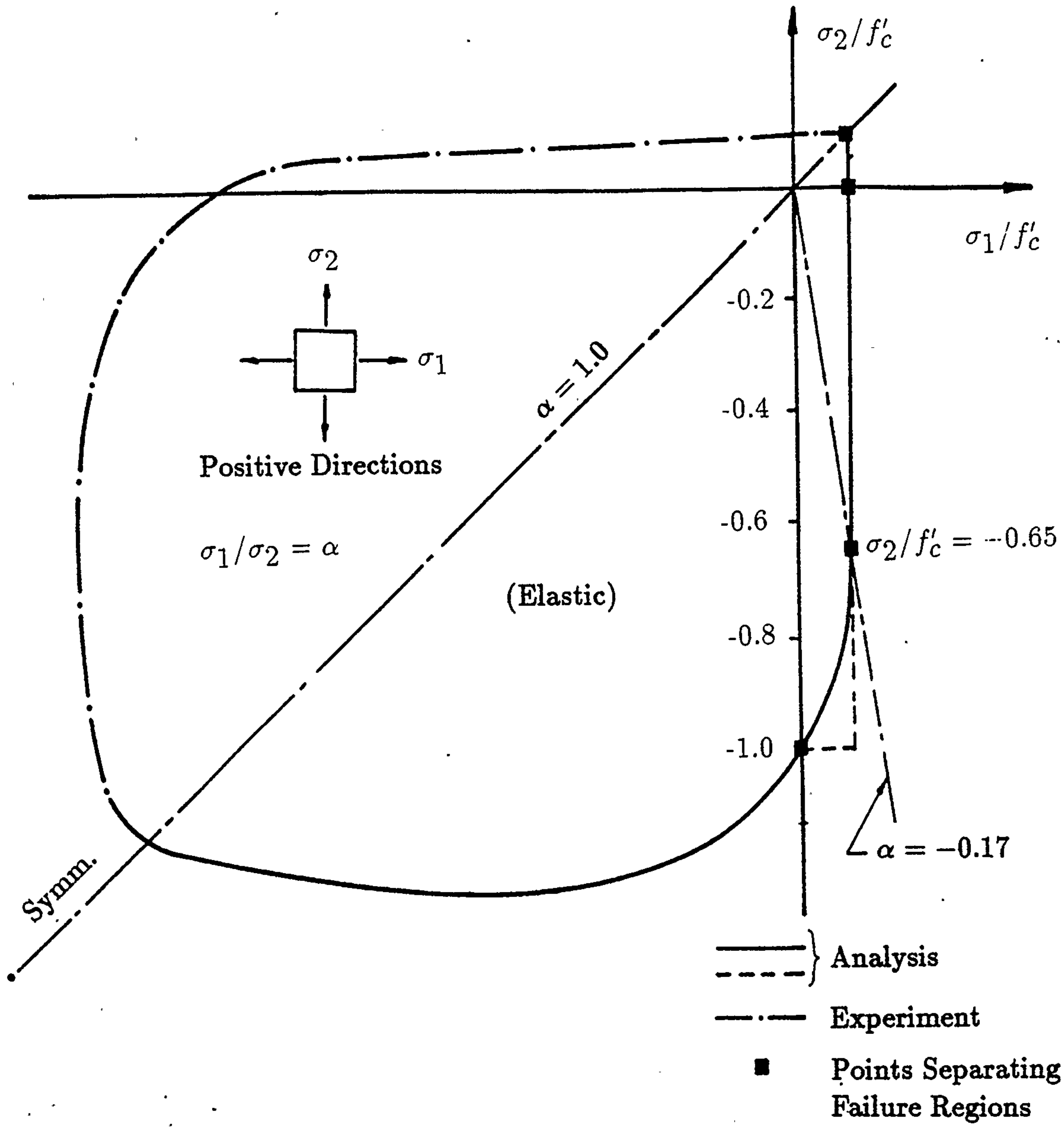

Figure 3.4: Biaxial Failure Envelope

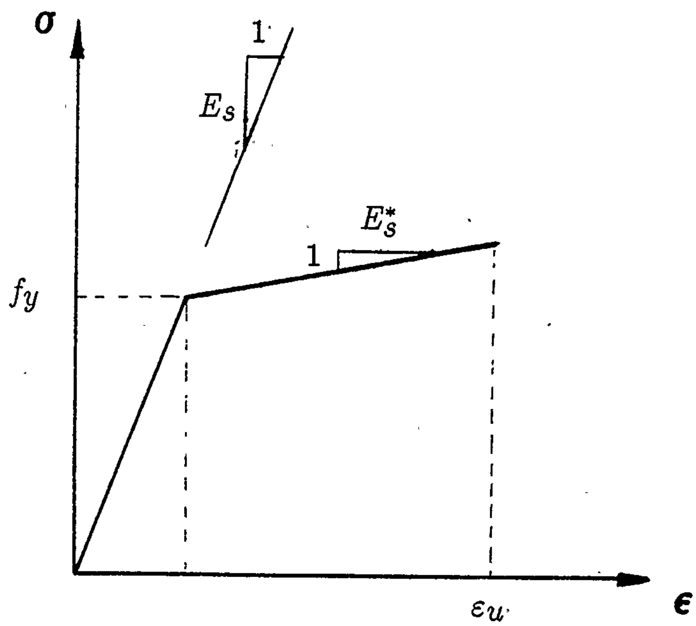

Figure 3.5: Steel Material Model

of box girders, and shells. The main feature of QLC3 is that the shape function for u is linear in x and y, but that for v is linear in y and cubic in x as shown in Figure 3.6. This allows the element to exactly model beam-like behaviour. The performance of the element when beam-like behaviour is not predominant was tested by Sisodiya (1971) and was found to be quite satisfactory.

3.4 Model Details

The basic model under examination is a two-dimensional in plane model using the QLC3 element. In all cases the member has a length of 1.0 m, height of 0.25 m and a width of 0.375 m. Symmetry is used to advantage and only half the member is actually modelled. Load is applied as shown in Figure 3.7. The load is applied

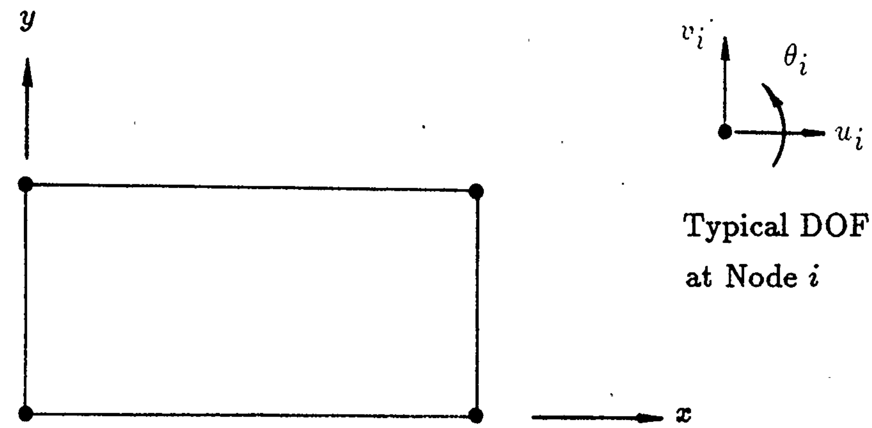

Figure 3.6: The QLC3 Finite Element

gradually and in all cases each load step corresponds to an increase of 0.1 MN. So, for example, load step 15 would correspond to a total applied load of 1.5 MN. The relevant concrete and steel properties are given in table 3.1. The variable β is a constant smaller than one to account for shear stiffness due to aggregate interlock and dowel action in cracked concrete.

3.5 Mesh Size and Integration Order

Prior to commencing the parametric study, it was necessary to gain an understanding of the effect of the mesh geometry and the element integration order on the results. A comparison of the three mesh geometries shown in Figure 3.8 was conducted. Figure 3.8 a, b, and c show a 12 element mesh, a 24 element mesh and a 72 element mesh of QLC3 type elements. In all cases there is no reinforcing steel whatsoever. Nodes on the left end of the mesh are restrained against horizontal translation and

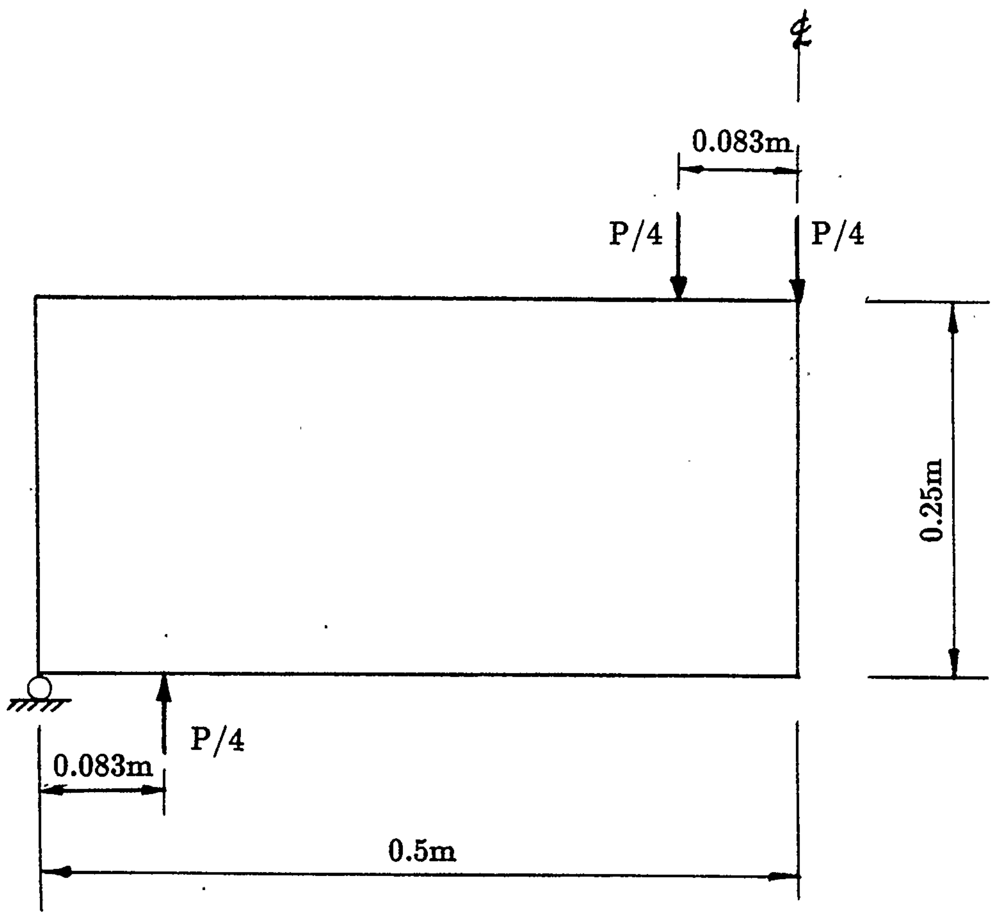

Figure 3.7: Load Application Points

Item	Value
f'_c	62.5 MPa
f_t	4.47 MPa
ε_{cu}	0.002
ε_{tu}	0.0048
E_0	40000 MPa
β	0
ν	0.15
f_y	265 MPa
E_s	200000 MPa
E_s^*	6693 MPa
ε_u	0.02

Table 3.1: Steel and Concrete Material Properties

in-plane rotation. Nodes on the the centre line are restrained in a similar fashion as required for symmetry. Only the bottom left node is restrained against vertical translation. This set of boundary conditions is referred to throughout this work as the 'Arch' support condition. A 2x2 Gaussian integration scheme is used to determine material states and to numerically integrate the element stiffness matricies. Loads are applied as detailed in Figure 3.7

Figure 3.9 shows the load plotted as a function of the centre line deflection for these three mesh geometries. It can be seen that the 12 element mesh behaves differently from the other two beyond a load level of 1.2 MN. An examination of the crack distributions at a load level of 1.4 MN shown in Figure 3.10 illustrates the reason for the difference. The inclined lines in the element represent the orientation of the cracks at each gauss point. The length of these lines has no significance. Recall that each load step corresponds to a load level of 0.1 MN. The 24 and 72 element meshes shown in Figure 3.8 have diagonal shear cracks throughout the middle part of the beam. These cracks make the mesh substantially more flexible than the 12 element

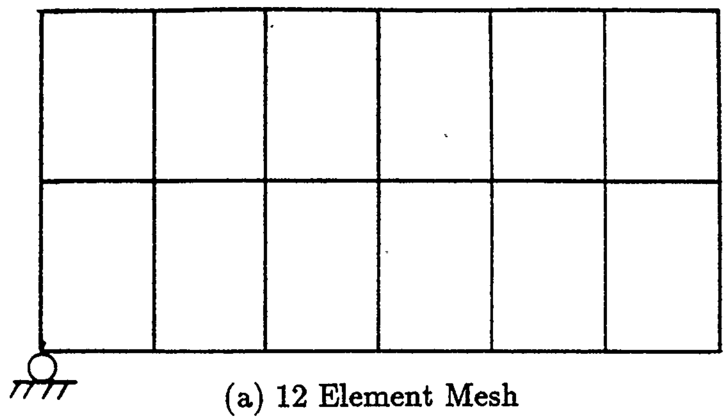

(a) 12 Element Mesh

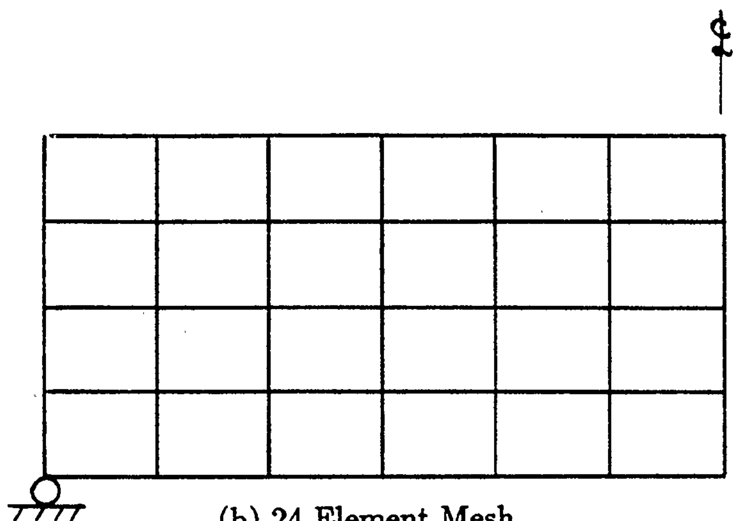

(b) 24 Element Mesh

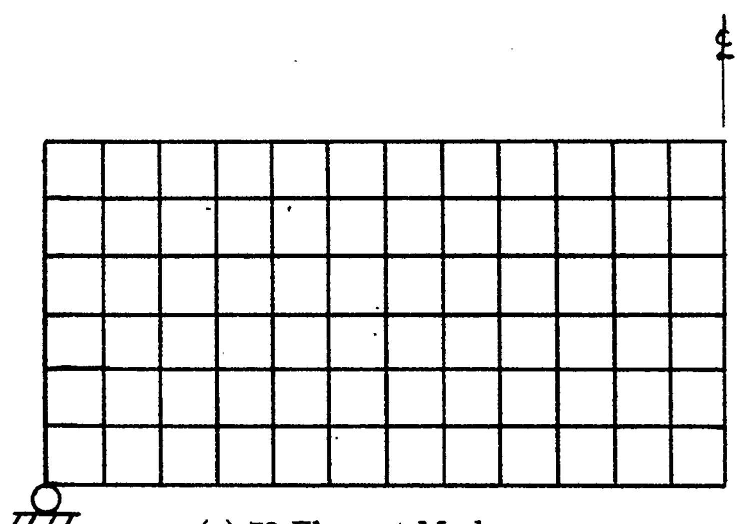

(c) 72 Element Mesh

Figure 3.8: Mesh Geometries

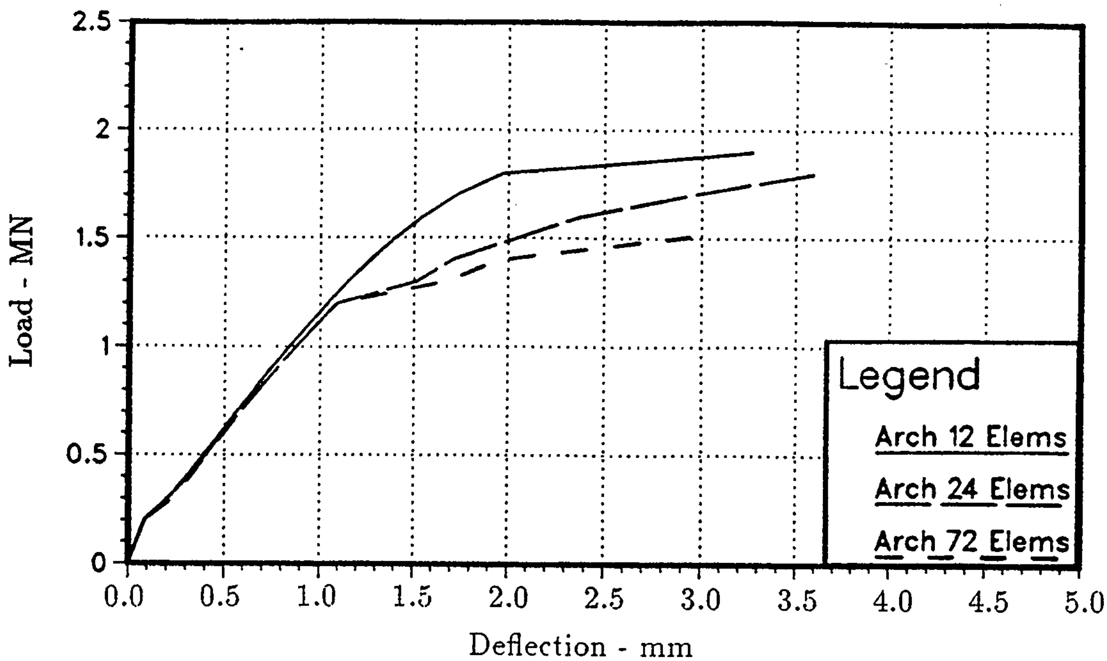

Figure 3.9: Comparison of Effect of Mesh Size - No Reinforcing Steel

mesh, which has no cracks other than the tension cracks shown in Figure 3.10a. The 12 element mesh is too coarse to model this important phenomenon, and is therefore inadequate for the analysis.

On the other hand, the 24 and 72 element meshes behave identically up to the 1.5 MN load level, at which point the 72 element mesh collapses. The 24 element mesh carries on to collapse at a load of 1.8 MN. Because the 72 element mesh is approaching the limit of the computer systems capabilities and is significantly more expensive to run, the 24 element mesh was selected for use in the remainder of the study.

The final decision to make is with regard to the order of integration. FELARC allows either a 2x2, 3x3, or 4x4 integration scheme to be used. The 24 element mesh was rerun using 3x3 integration and the resulting load deflection curve is plotted,

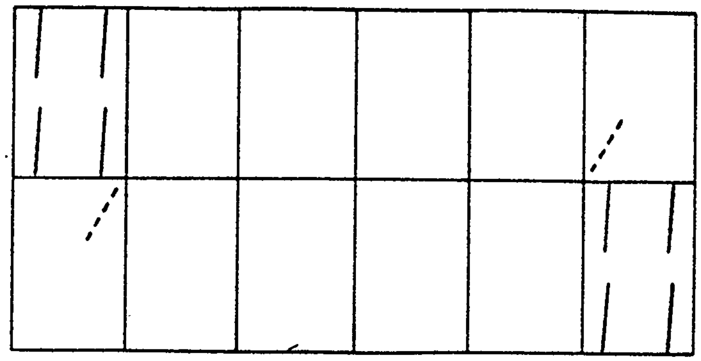

(a) 12 Element Mesh

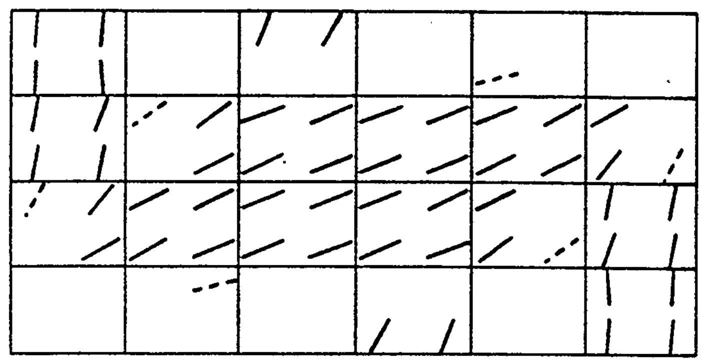

(b) 24 Element Mesh

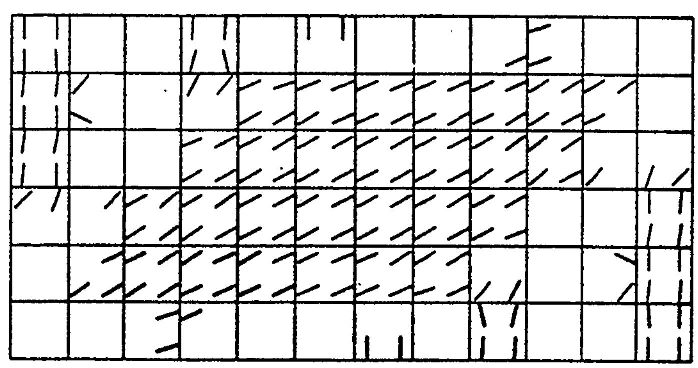

(c) 72 Element Mesh

Figure 3.10: Crack Distributions at Load Step 14 (P = 1.4MN)

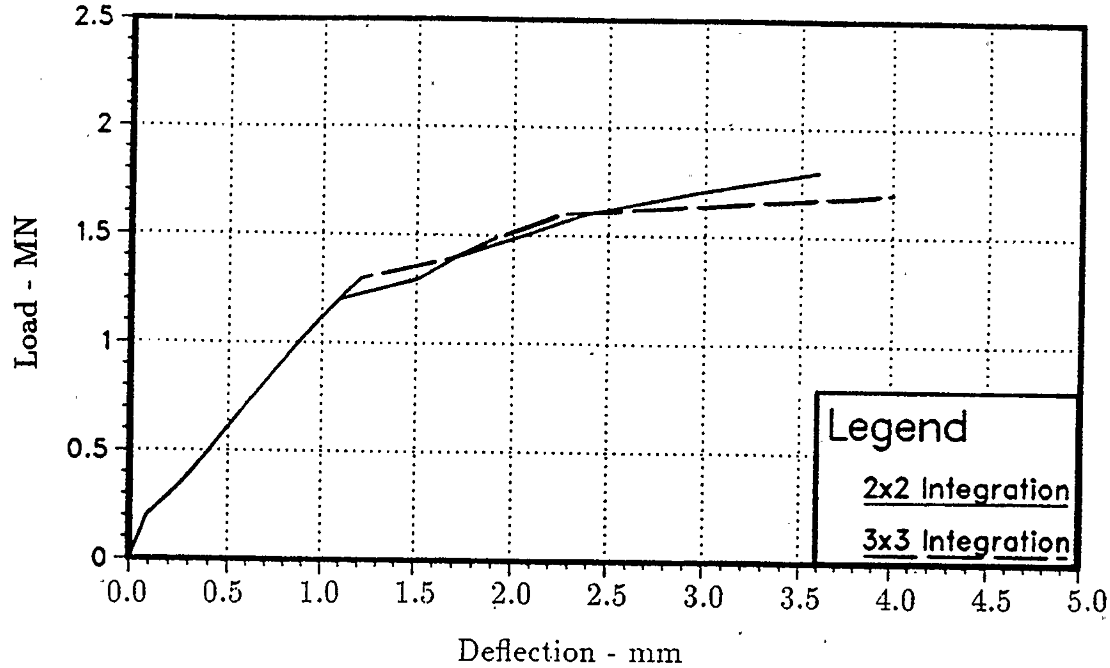

Figure 3.11: Comparison of Effect of Integration Order - No Reinforcing Steel

along with the 2x2 integration, in Figure 3.11. Although the mesh with 3x3 integration collapsed at a slightly lower load, the behaviour is almost identical up to this point. Therefore, it is concluded that 2x2 integration is adequate for the task, and the extra expense of 3x3 integration is not required.

The element and node numbering scheme for the 24 element mesh is presented in Figure 3.12.

3.6 Parameters Investigated

Two principal parameters are investigated. Firstly, the effect of varying the lateral support stiffness was examined, and secondly, the amount and location of longitudinal reinforcing steel was considered.

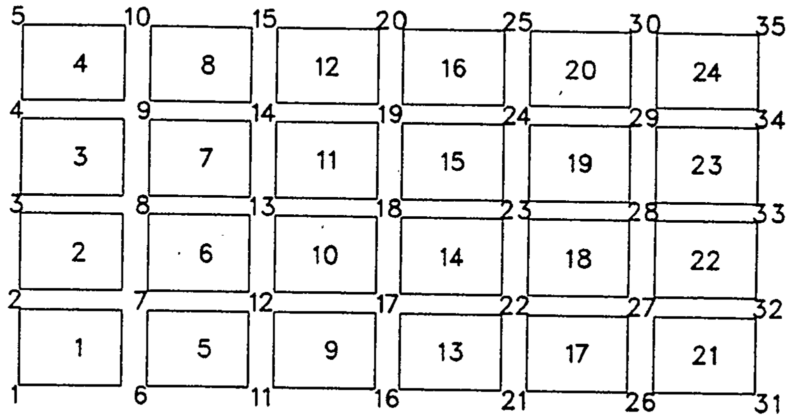

Figure 3.12: Node and Element Numbers - 24 Element Mesh

Three lateral support conditions are examined as shown in Figure 3.13. Figure 3.13a shows the case of full in-plane restraint in which the nodes on the boundary are completely restrained against translation in the horizontal direction and rotation about the out of plane axis. As discussed previously, this is referred to as the "Arch" condition. Figure 3.13b shows the restraint condition referred to as "Spring 1". The sum total of the horizontal spring stiffnesses is equal to that of a 1.0 m long concrete beam restrained laterally at its opposite end. Put another way, the springs are intended to simulate the stiffness of second 1.0 m span of the beam which is continuous with the first span, and is horizontaly restrained at its opposite end. The stiffness of each spring is calculated using $K = Ea/l$ where E, the stiffness of the concrete, is 40000 MPa, a, the cross sectional area, is calculated by multiplying the width of the element (0.375m) times the height of each element (.0625 m or half of this for the outside elements), and l is 1.0. This allows the boundary of the span under investigation some degree of flexibility, but it is probably less stiff than the real situation. For this reason, a third boundary condition referred to as "Spring 2" was developed. This case is similar to Spring 1 in that there are springs in the same locations, but each spring is ten times as stiff as the spring 1 condition as shown in Figure 3.13c. In both the Spring 1 and Spring 2 cases the nodes where the beam is attached to the springs are restrained against rotation about the out of plane axis.

Four arrangements of longitudinal reinforcing steel are examined as shown in Figure 3.14. The first arrangement is unreinforced as shown in Figure 3.14a. This case is included as a base case to establish the capacity of the concrete core in absence of any steel. The second arrangement consists of 2.6% (a 6.25 mm plate) reinforcing steel on the bottom surface of the member, as shown in Figure 3.14b. This arrangement may be considered to have short shear studs projecting from the steel into the concrete. This is due to the fact that no slip is allowed to occur between the steel plate and the concrete. The third arrangement has 2.6% reinforcing on the top and bottom surfaces as shown in Figure 3.14c. The final arrangement, shown in Figure 3.14d is identical to the previous case except for the addition of two 6.25 mm diaphragms. This arrangement corresponds to the beams used in the experimental work of Zimmerman (1987).

Each of the four steel arrangements is combined with each of the three end support conditions, resulting in 12 combinations. In addition, several other models were formulated. The diaphragms connecting the top and bottom plates are basically a type of shear connector. An alternative method of shear connection is to attach long stud shear connectors to each plate. The arrangement of studs as shown in Figure 3.15 is examined and the results compared to the model with diaphragms. The area of each stud is 586 mm^2 (equivalent to a 27.3 mm diameter bar) and the total amount of steel in the studs is equal to the amount of steel in the diaphragms.

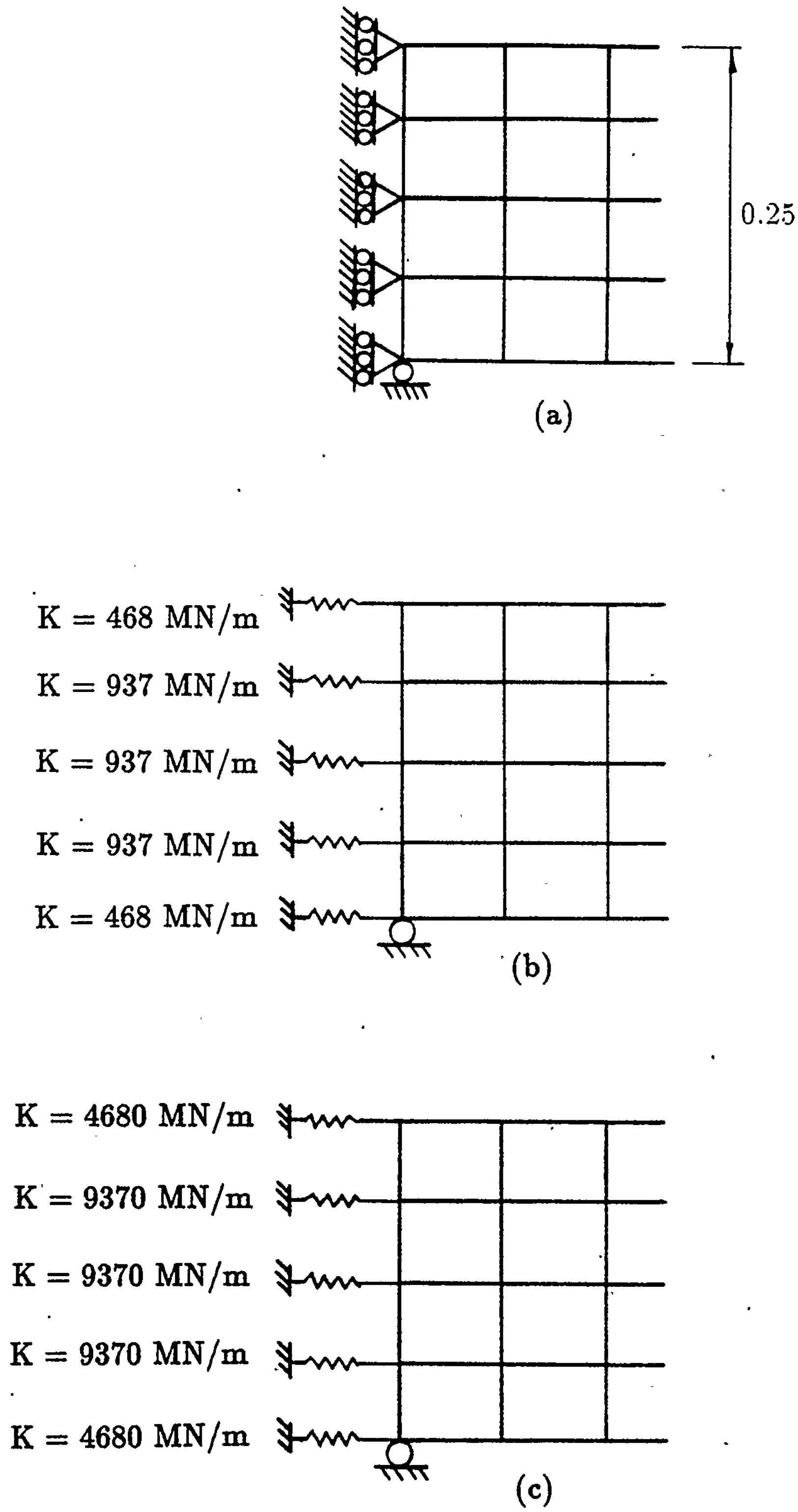

Figure 3.13: End Support Conditions

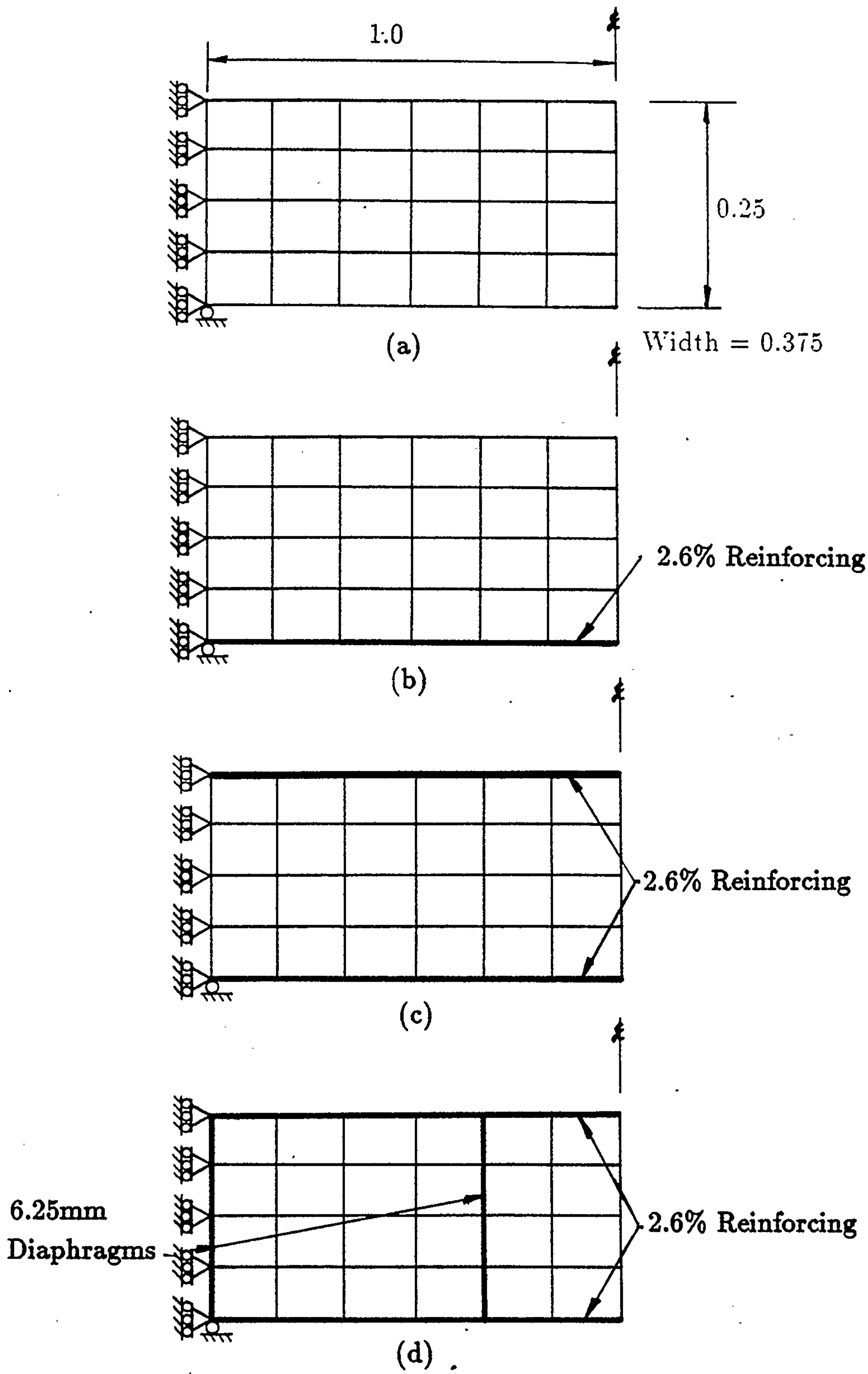

Figure 3.14: Arrangement of Longitudinal Reinforcing Steel

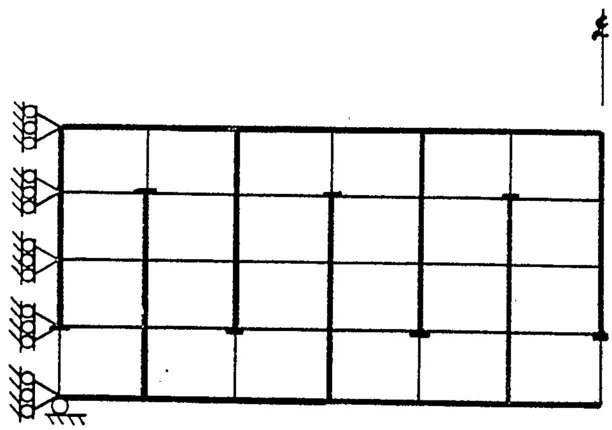

Figure 3.15: Arrangement of Long Shear Stud Connectors

Another model considered is a three span beam with a point load in the middle span as shown in Figure 3.16. The intention of this model is to compare the results of the simulated three span models, Spring 1 and Spring 2, with the actual three span case. Only the case with 2.6% reinforcing top and bottom was considered.

Finally, a model with a length of 2.0 m, and a span to depth ratio of 8 was formulated. The mesh is illustrated in figure 3.17. This model was run with all four steel arrangements, but only for the Arch support condition.

3.7 Discussion of Results

3.7.1 Base Case

The model with the supports fully restrained against in-plane deflection (the Arch support condition) and completely unreinforced is considered to be the base case.

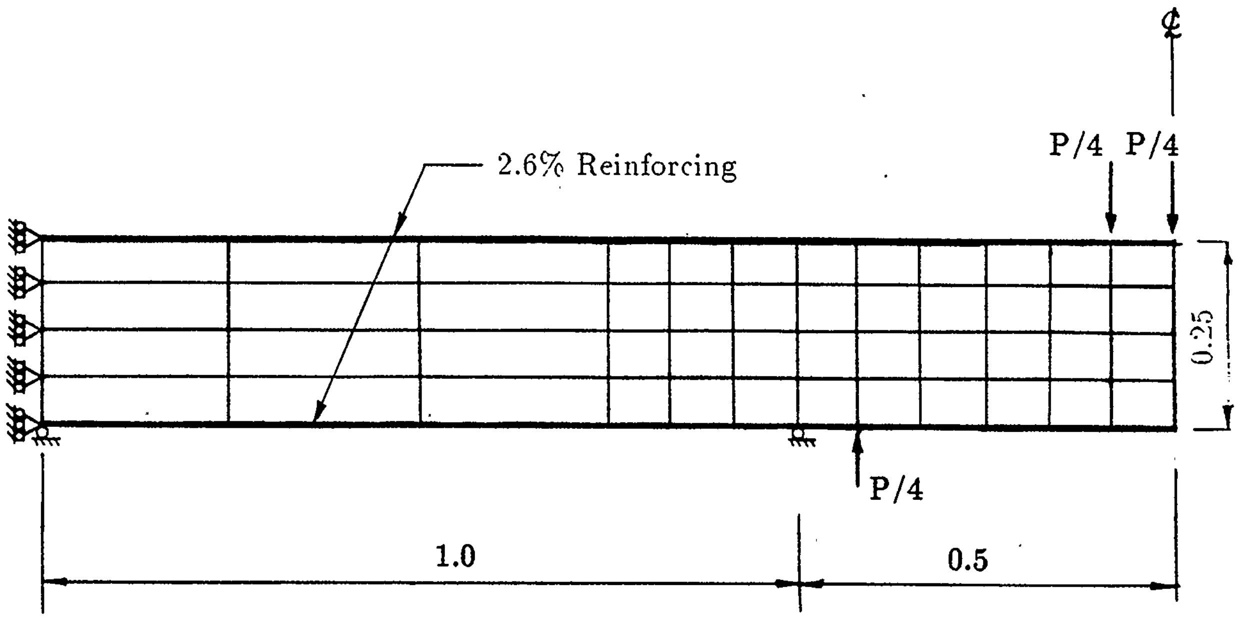

Figure 3.16: Three Span Beam

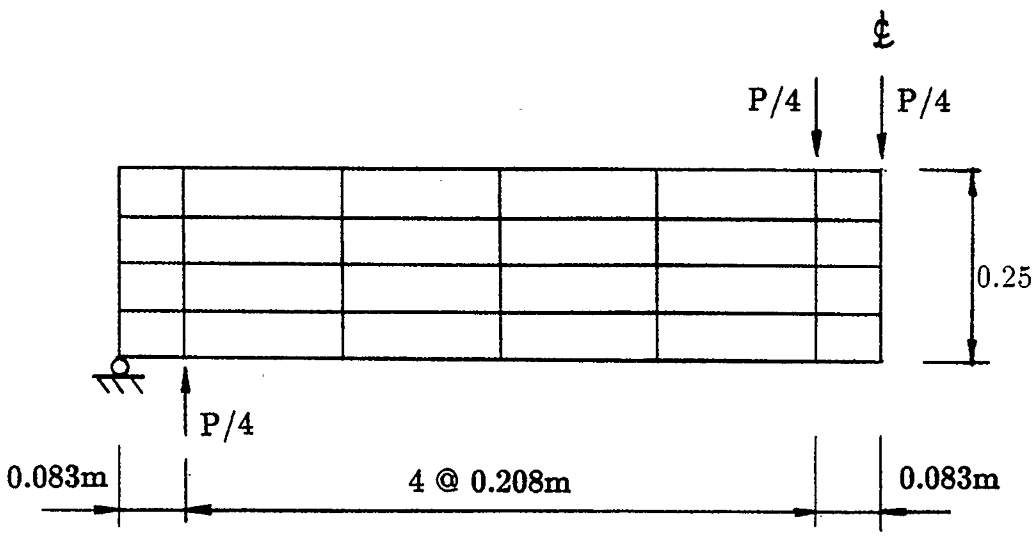

Figure 3.17: Beam with Span to Depth Ratio of 8

The maximum load carried at collapse was 1.8 MN with a centre line deflection of 3.5 mm. Failure was by crushing of the concrete at the top directly under the load and at the bottom directly over the supports (ie. the nodes), simultaneously.

The maximum expected load calculated using the simple strut theory formulated in section 3.2 is 1.5 MN. This occurs at a deflection of 4.25 mm. As expected for the reasons discussed in the introduction of the strut theory, the deflection of the finite element model is less than that predicted by the strut theory. The maximum load calculated by the finite element model is greater than that calculated by the strut theory. Interestingly though, the maximum load calculated using the 72 element mesh was 1.5 MN, the same value as predicted by the strut theory.

It is also interesting to note that if this were an unreinforced continuous beam, the collapse load, based on first cracking, would be approximately 0.14 MN. This is based on beam theory which is not strictly applicable because the span to depth ratio is so small. However, this means that compressive membrane action provides an increase of approximately 12 times in the load carrying capacity.

The results of the finite element analysis in the form of plots of the deformed mesh, the principal compression vectors, and the crack orientations for selected load steps are presented in Figures 3.18 to 3.20. The first cracks developed between load step 2 and 3 in which the applied load was between 0.2 and 0.3 MN. The crack pattern for this load level is the same as load step 4, which is illustrated in Figure 3.20. Note that solid lines imply that at the integration point, the tensile strain exceeded the tension stiffening range of the material and the concrete has completely cracked. A dashed line means that the material at the integration point is still in the tension stiffening range, ie. cracked but still carrying some load in tension. The crack pattern remains unchanged as the load level increases to 1.4 MN (load step 14), at which point cracks parallel to the compression strut caused by Poisson's effect suddenly appear. After this occurrence, the member becomes less stiff.

Figure 3.18 shows the deformed mesh plots for selected load steps. Deformations are plotted with a distortion factor of 25, which means that they are plotted to a scale 25 times smaller the the undeformed mesh. It can be seen that the member has no horizontal displacement at the support or at the centre line as imposed by the support conditions.

The formation of the compression strut as the load is increased is seen clearly in Figure 3.19. The principal compression stress vectors are scaled so that 100 MPa is equal to the length, in the horizontal direction, of one element. After the formation of the diagonal cracks at load step 14, the compression strut becomes somewhat narrower. Finally, the member fails by crushing of the concrete at the upper right and lower left corners (ie. the two compression nodes) simultaneously.

3.7.2 Effect of Support Stiffness

The effect of the in-plane support stiffness was examined by replacing the horizontal fixity with horizontal springs as discussed previously in section 3.6

Figures 3.21 to 3.24 show the applied load as a function of the centre line deflection for the four arrangements of longitudinal steel. With all reinforcements, the two spring supported cases are more flexible and carry less load at collapse than the rigidly supported case. Table 3.2 summarizes the results of the load carrying capacity of each case. Both the absolute load at collapse, in MN, and the load expressed as a percent of the arch case are tabulated. The results for each steel arrangement

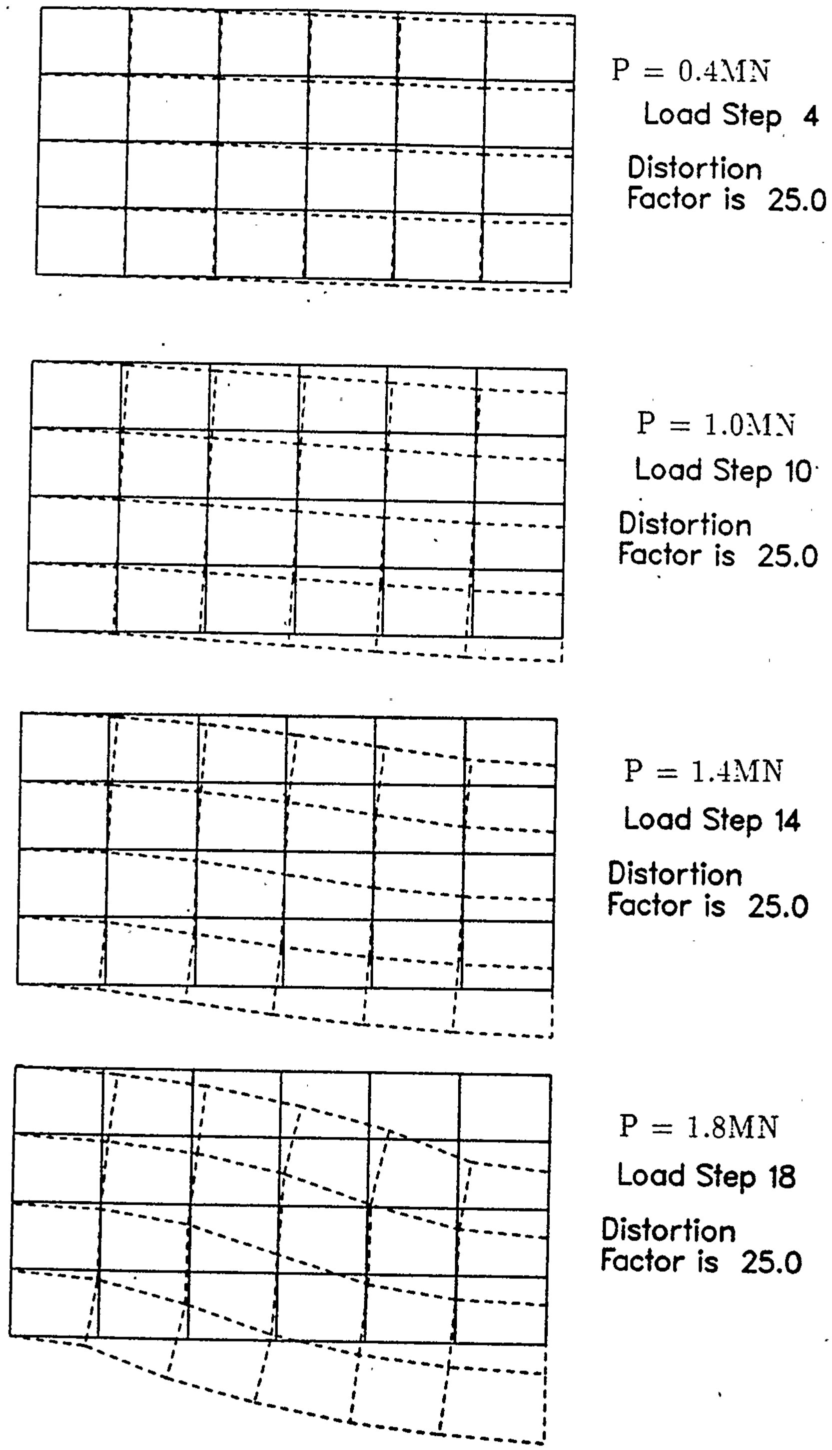

Figure 3.18: Base Case Deformed Mesh

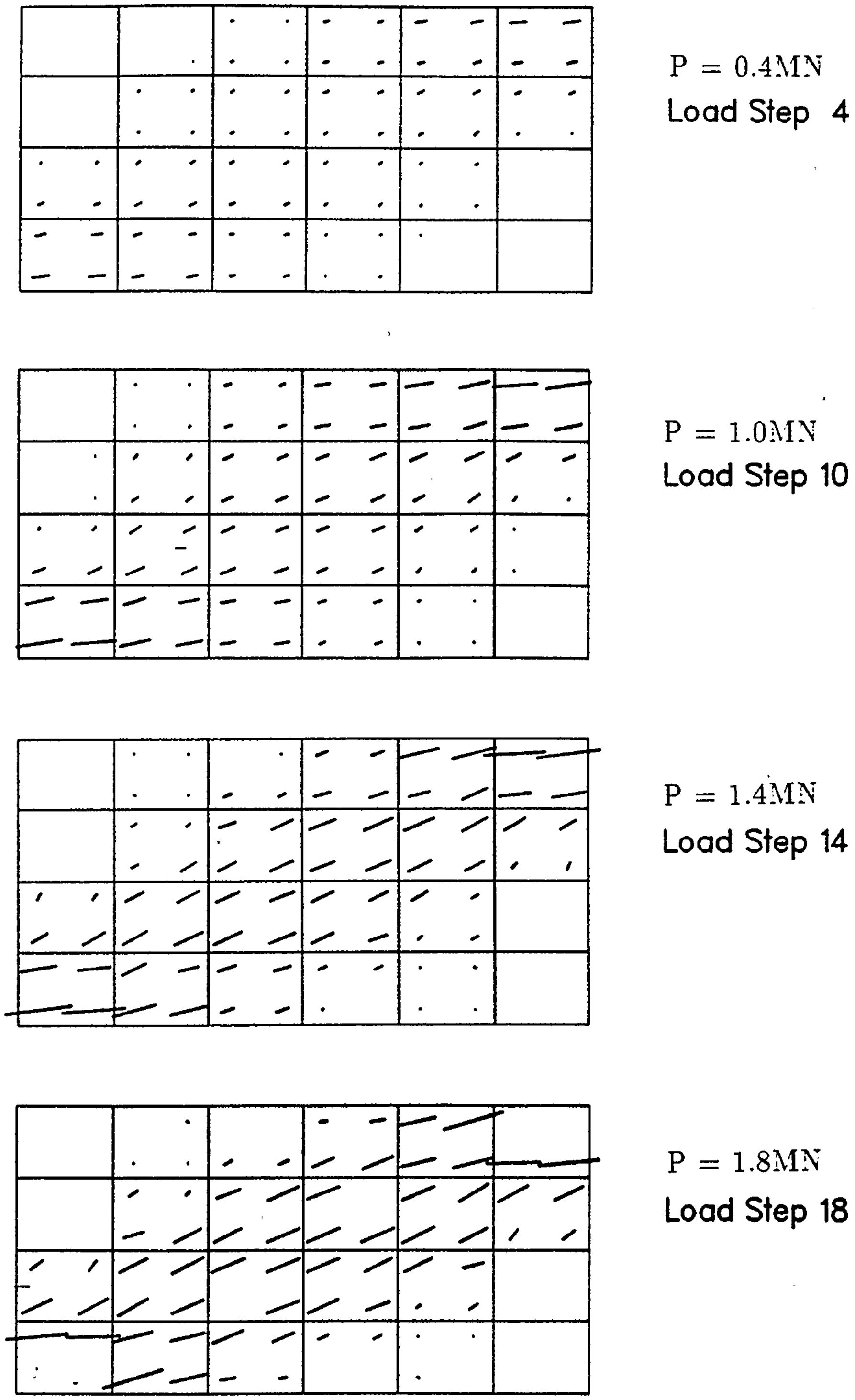

Figure 3.19: Base Case Principal Compressive Stress

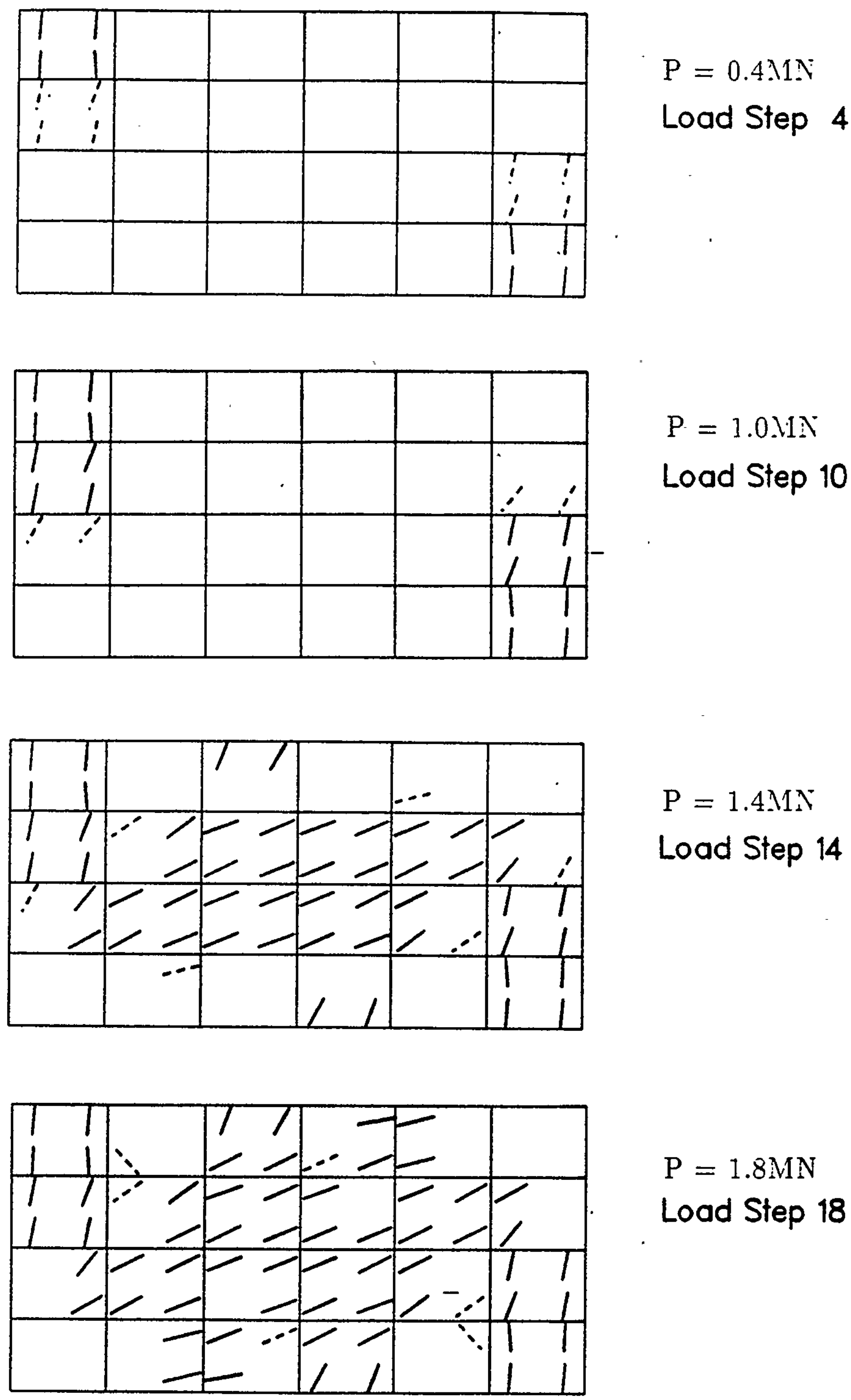

Figure 3.20: Base Case Crack Orientation

Steel Arrangement	Support Condition		
	Arch	Spring 1	Spring 2
No Steel	1.8 MN	1.3 MN - 72%	1.7 MN - 95%
2.6% Bottom	1.7 MN	1.1 MN - 64%	1.7 MN - 100%
2.6% Top and Bottom	2.2 MN	1.5 MN - 68%	1.9 MN - 86%
2.6% Top and Bottom With Diaphragms	2.4 MN	1.6 MN - 66%	2.2 MN - 91%

Table 3.2: Load Capacity - Absolute and as a Percent of the Arch Case

are quite consistent. The Spring 1 support condition carries 64% to 72% of the Arch support condition, and Spring 2 carries 86% to 100% of the Arch condition.

Figure 3.25 shows the deformed mesh plots at load step 12 (P=1.2 MN) for the no steel case for each support condition. The effect of the spring stiffness on the amount of end rotation and centre line deflection is clearly seen.

Figure 3.23 contains a fourth support condition labeled "Three Span". This is the model that actually is a three span beam as discussed in section 3.6 and illustrated in Figure 3.16. The load deflection curve for this case falls almost exactly midway between the curve for Spring 1 and Spring 2. The collapse load for this case is 1.9 MN, which is 86% of the Arch condition. For the given load conditions the collapse load of the Arch support condition is a fairly close approximation of that of a three span beam.

3.7.3 Effect of Steel Arrangement

Various steel arrangements as discussed in section 3.6 are examined. The plots of applied load as a function of centre line deflection for each support condition are shown in Figures 3.26 to 3.28. In all cases the member is slightly more stiff as more steel is added. In all but one case the member carries slightly more load prior to

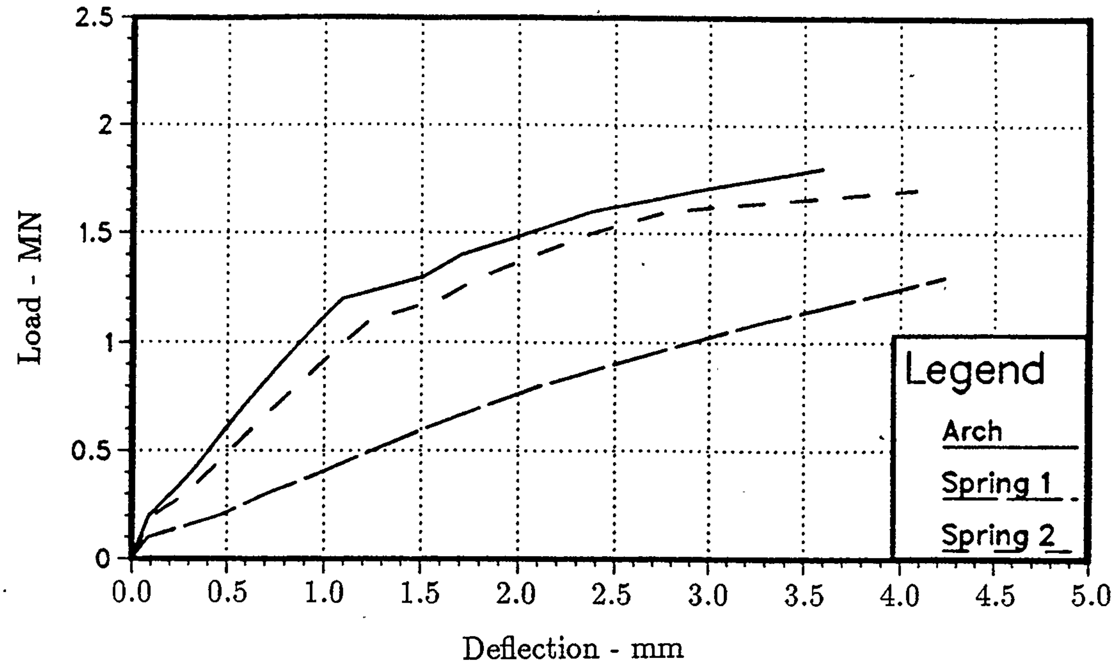

Figure 3.21: Comparison of Effect of Support Stiffness - No Reinforcing Steel

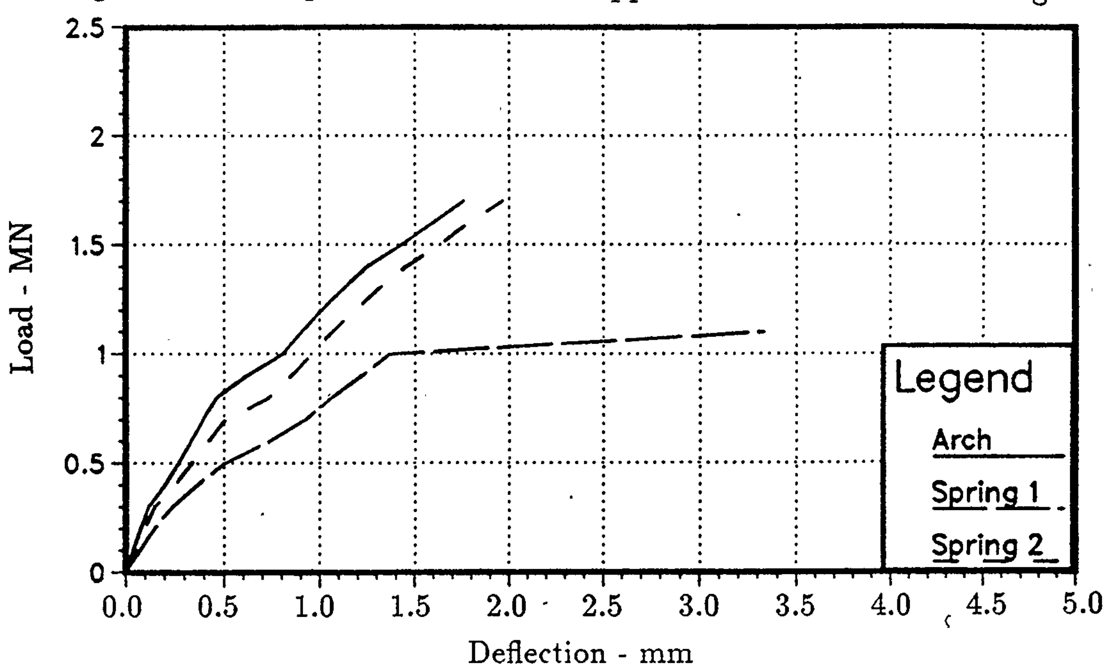

Figure 3.22: Comparison of Effect of Support Stiffness - 2.6% Reinforcing Steel Bottom

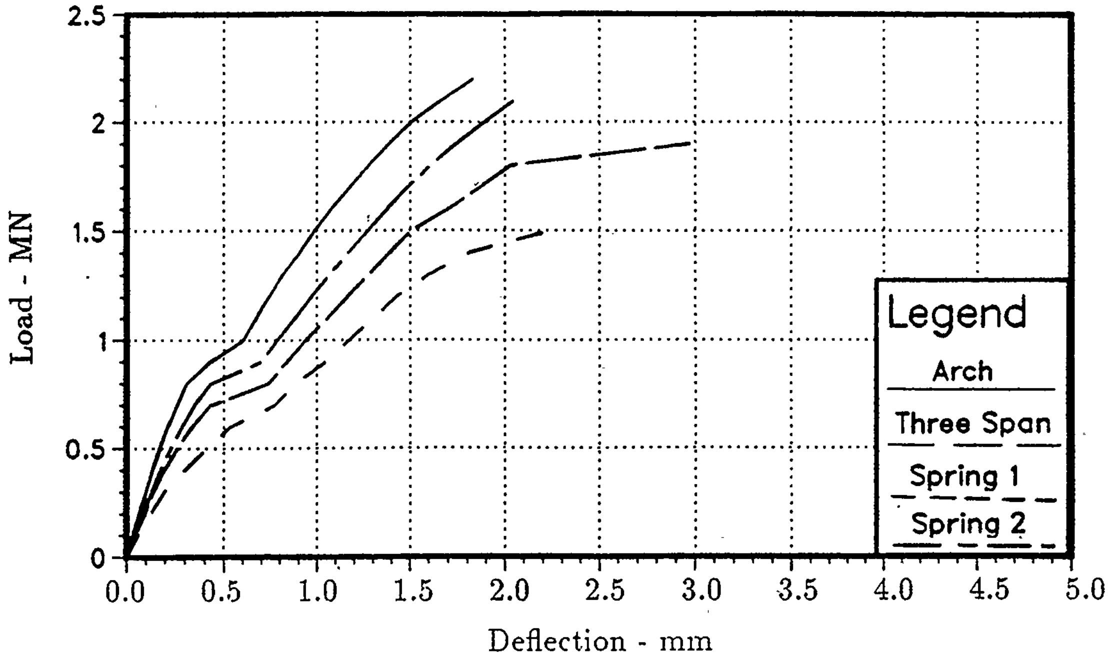

Figure 3.23: Comparison of Effect of Support Stiffness - 2.6% Reinforcing Steel Top and Bottom

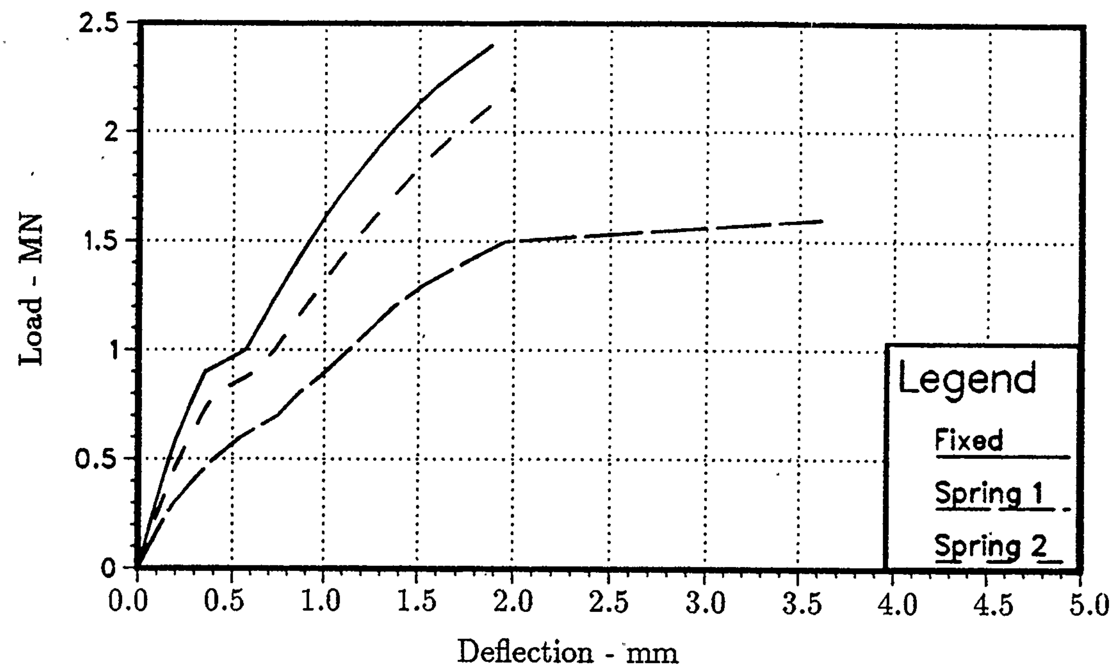

Figure 3.24: Comparison of Effect of Support Stiffness - 2.6% Reinforcing Steel Top and Bottom with Diaphragms

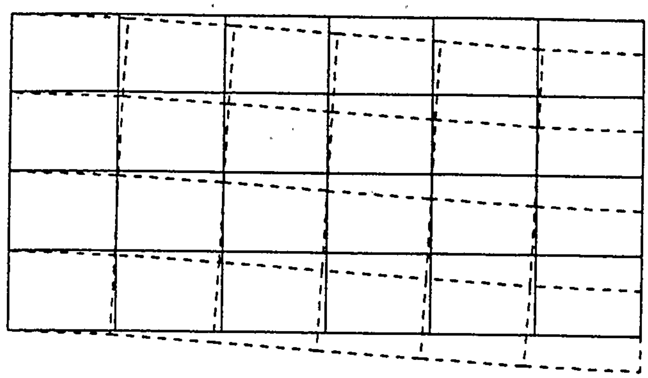

(a) Arch Support

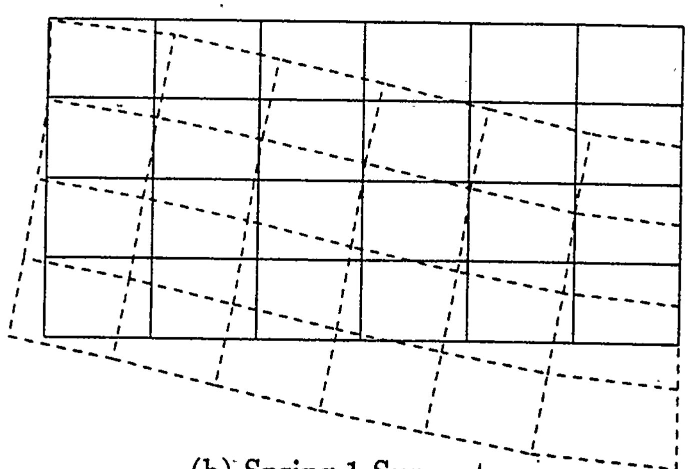

(b) Spring 1 Support

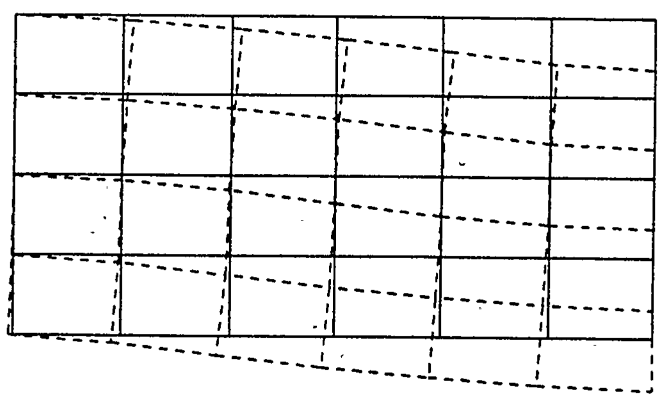

(c) Spring 2 Support

Figure 3.25: Deformed Mesh at Load Step 12, No Steel Case (P = 1.2 MN)

Steel Arrangement	Support Condition		
	Arch	Spring 1	Spring 2
No Steel	1.8 MN	1.3 MN	1.7 MN
2.6% Bottom	1.7 MN - 94%	1.1 MN - 85%	1.7 MN - 100%
2.6% Top and Bottom	2.2 MN - 122%	1.5 MN - 115%	1.9 MN - 112%
2.6% Top and Bottom With Diaphragms	2.4 MN - 133%	1.6 MN - 123%	2.2 MN - 129%

Table 3.3: Load Capacity - Absolute and as a Percent of the No Steel Case

collapse as more steel is added. The exception is the case with 2.6% steel on the bottom surface only. Table 3.3 summarizes the load carrying capacities of each case. Both the absolute load at collapse, in MN, and the load expressed as a percent of the no steel case are tabulated.

For all three support conditions, the case with 2.6% reinforcing steel on the bottom surface collapsed at or just below the load level supported by the no steel case. This may have been caused by a real phenomenon, or may have been caused by some aberration of the numerical simulation. The latter is likely the case because it is difficult to imagine that the load carrying capacity of the member could possibly decrease as steel is added. Part of the discrepancy may be due to the size of the load step. In these analyses the step size is 0.1 MN, and therefore actual differences in the ultimate load carrying capacity less than 0.1 MN will not be discernable. Load steps less than 0.1 MN would have helped to resolve the exact collapse load.

For all support conditions, the effect of significant amounts of reinforcing steel is almost negligible. The addition of 2.6% reinforcing steel top and bottom provides an increase of only 15% to 23% in the load carrying capacity, depending on the support condition. Inclusion of diaphragms increases the capacity only by an additional 6% to 11%. The reason for this behaviour is that the member is governed primarily by

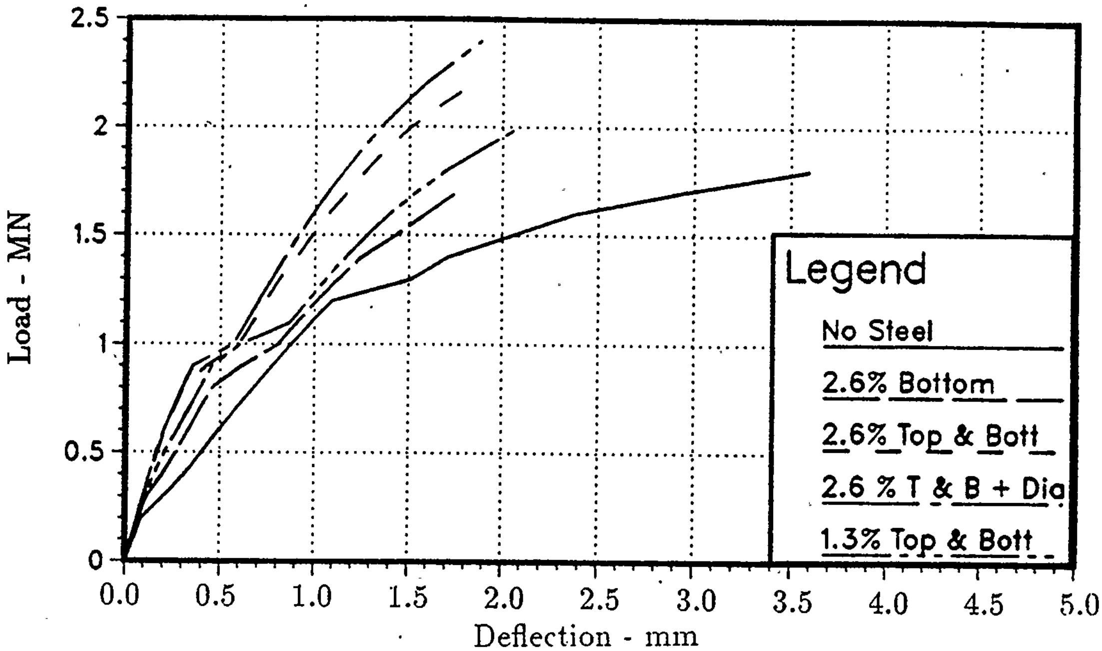

Figure 3.26: Comparison of Effect of Steel Arrangement - Ends Fully Restrained

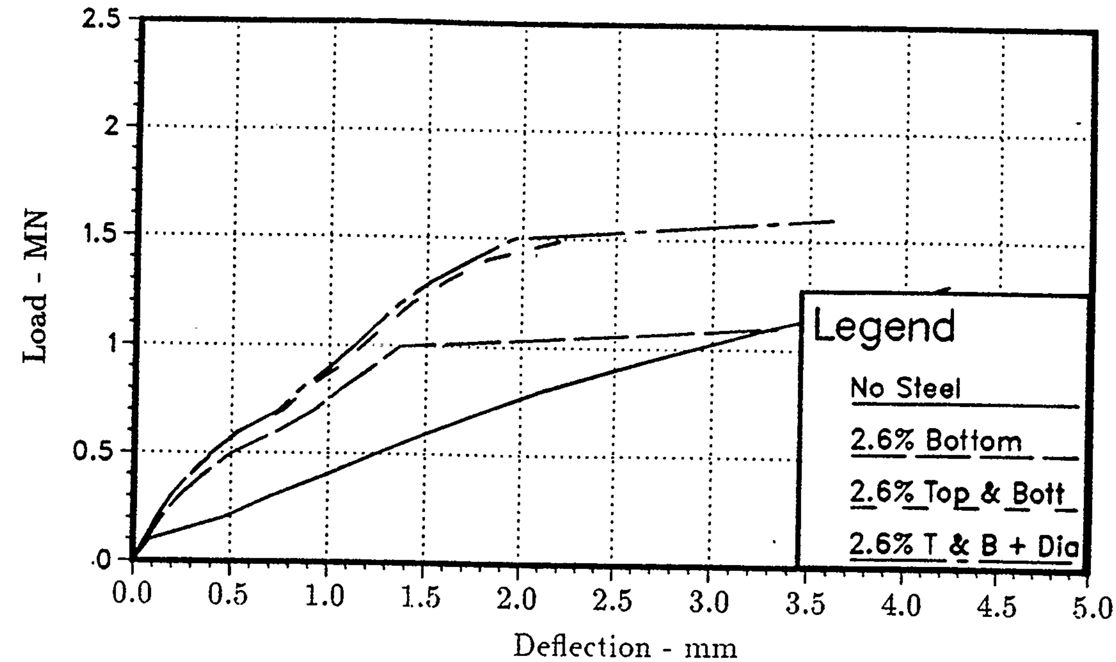

Figure 3.27: Comparison of Effect of Steel Arrangement - Ends Partially Restrained with Spring 1

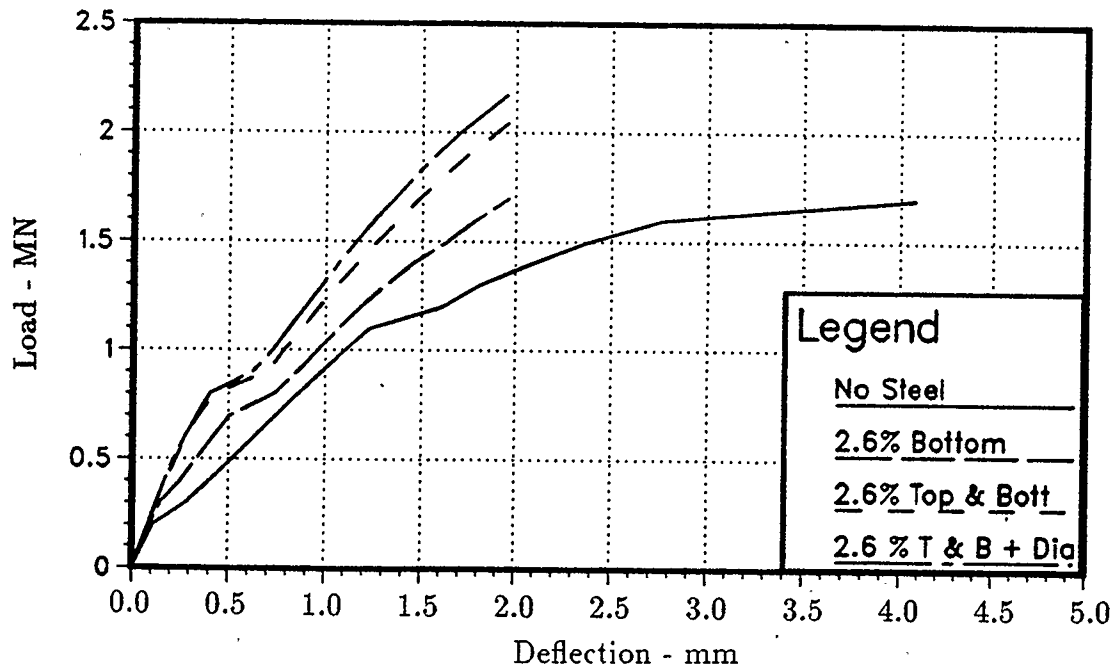

Figure 3.28: Comparison of Effect of Steel Arrangement - Ends Partially Restrained with Spring 2

the capacity of the concrete arch. The tension steel is virtually redundant in the load carrying mechanism because the horizontal component of thrust is provided by the support directly, rather than by the tension steel transfering the thrust to the opposite end of the member, as would occur with a tied arch member.

The addition of both tension and compression steel has the effect of subtly altering the shape of the compression strut as illustrated in Figure 3.29. Figure 3.29a shows the principal compression stress vectors at load step 16 (P = 1.6 MN) for the no steel Arch support case. Figure 3.29b shows the corresponding plot with 2.6% reinforcing steel top and bottom. The compression strut is about the same width in both cases, but in the latter case the stresses are almost constant in magnitude through the entire strut. In the no steel case the compression vectors flatten out and become larger in magnitude in the upper right and lower left corners, but this does not occur in the latter case.

Figure 3.29c shows the corresponding plot with diaphragms included. It appears to be almost identical to Figure 3.29b, with the possible exception that the compression stresses are even more constant in magnitude through the entire strut.

Figure 3.30a and b show the principal compression stress vectors at load step 20 (P = 2.0 MN) for the cases with 2.6% reinforcing steel top and bottom, without and with diaphragms respectively. It can be seen that the influence of the diaphragms manifests itself primarily in the magnitude of the compression stresses in element 16 and, to a lesser extent, element 18 (refer to Figure 3.12).

These concepts apply also to the two other support conditions, Spring 1 and Spring 2.

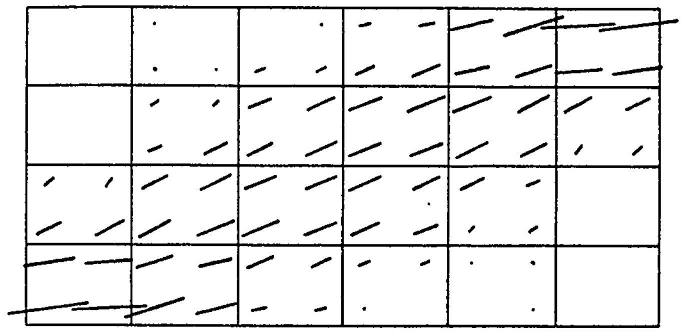

(a) No Steel

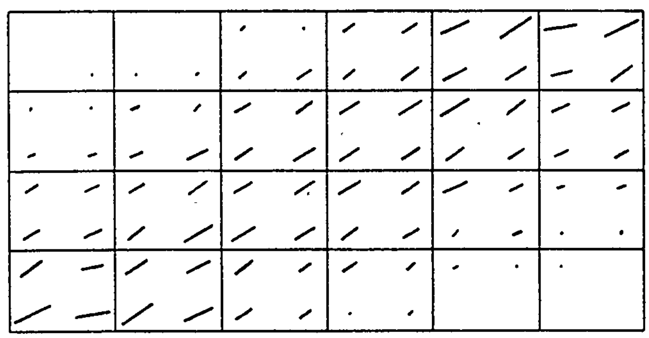

(b) 2.6% Reinforcing Top And Bottom

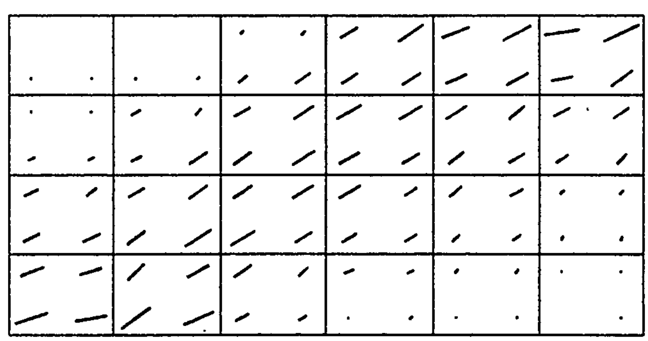

(c) 2.6% Reinforcing Top and Bottom Plus Diaphragms

Figure 3.29: Principal Compressive Stress Vectors at Load Step 16 - Arch Support (P = 1.6 MN)

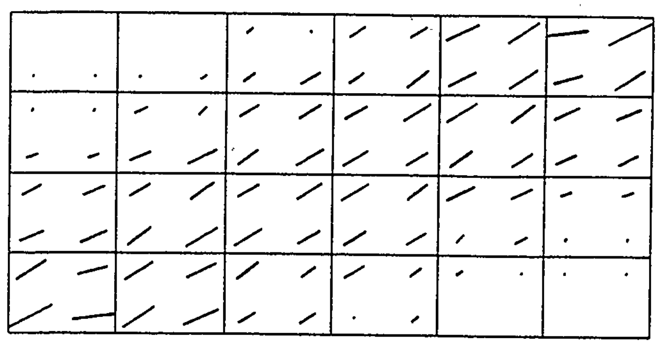

(a) 2.6% Top and Bottom Reinforcing

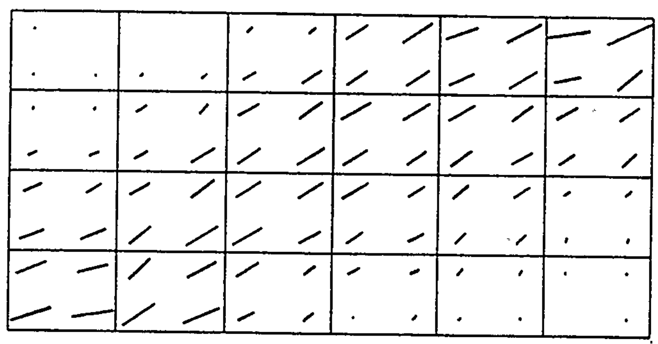

(b) 2.6% Top and Bottom Reinforcing Plus Diaphragms

Figure 3.30: Principal Compressive Stress Vectors at Load Step 20 - Arch Support (P = 2.0 MN)

3.7.4 Effect of Shear Connectors

The effect of the shear stud arrangement introduced in section 3.6 is examined. The basic mesh (labeled "Arch" on figure 3.31) is the Arch support case with 2.6% reinforcing both top and bottom. It should be noted that this case, which has no additional shear reinforcing, can be considered to have regular (ie. short) shear studs at regular spacing. This is because of the connection of the steel and concrete to common nodes with no allowance for slip between the two surfaces. The second mesh (labeled "Diaphragms") is similar to the first with the addition of diphragms as indicated in figure 3.14d. The third mesh (labeled "Long Studs") is similar to the first with the addition of long shear studs as indicated in figure 3.15.

It can be seen in figure 3.31 that studs and diaphragms have almost the same effect, the load-deflection curves being virtually superimposed on one another. Both cases are just marginally stiffer than the case with no additional shear steel. The mesh with long studs failed at a load of 2.0 MN because of convergence difficulties. In this particular case the numerical solution procedure failed, rather than the structure. The unbalanced loads oscillated about the equilibrium position with ever increasing magnitude until eventually the divergence criteria were exceeded and it was necessary to abort the analysis. Repeated attempts to cure this problem met with failure. In all probability had this problem not occurred the mesh would have sustained the same amount of load as the mesh with diaphragms.

3.7.5 Effect of Span to Depth Ratio

The effect of span to depth ratio was examined by increasing the lenth of the beam to 2.0 m, and keeping the depth constant at 0.25 m. This results in a span to

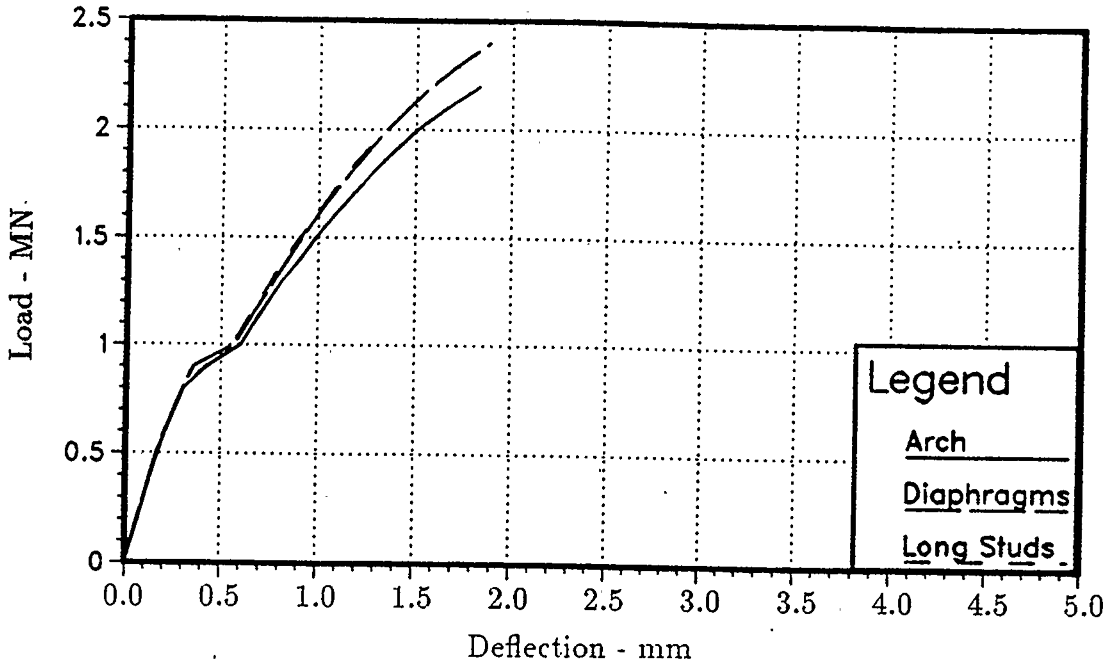

Figure 3.31: Comparison of Effect of Various Types of Shear Reinforcing - Arch Support

Steel Arrangement	Span to Depth 4	Span to Depth 8	
	MN	MN	% of S/D=4
No Steel	1.8 MN	0.9 MN	50%
2.6% Bottom	1.7 MN	0.9 MN	50%
2.6% Top and Bottom	2.2 MN	1.1 MN	50%
2.6% Top and Bottom With Diaphragms	2.4 MN	1.2 MN	50%

Table 3.4: Comparison of Load Capacities for Span to Depth Ratio 8 and 4

depth ratio of 8, double that of the previous analysis. All four steel arrangements in combination with only the Arch support condition were analysed. In all four cases the ultimate load carrying capacity decreased by a factor of two, as illustrated in table 3.4

Note that the analytical strut model discussed in Section 3.2 predicts a capacity of 0.75 MN for the unreinforced case, which is exactly 50% of the capacity calculated using this model with a span to depth ratio of 4.

Chapter 4

Three Dimensional Analysis

4.1 Introduction

A three dimensional finite element analysis has been conducted in order to compare and contrast the results with those of the two dimensional analysis. Specifically, the assumptions made regarding the boundary conditions in the two dimensional analysis will be examined. Several commercially available finite element programs including ABAQUS, ADINA, and ANSYS were investigated prior to selecting ANSYS for use in this study.

The ANSYS program was selected primarily because it had been shown to be successful in similar analyses, and because of the sophisticated graphical presentation the program is capable of. The computer program used for the two dimensional analysis, FELARC, was not suitable for this three dimensional analysis. Although FELARC has a three dimensional shell element, it is based on thin plate bending theory, which assumes that a normal to the surface of the plate remains normal after deformation. This assumption is acceptable for thin plate problems in which bending effects dominate, but is totally unacceptable for cases where shear effects dominate the solution. Because the span to depth ratio of the slab under consideration in this study is so small, shear effects will dominate, and an analysis based on thin plate theory will deliver erroneous results.

4.2 The ANSYS Program

ANSYS is a powerful, commercially available suite of finite element programs developed by Swanson Analysis Systems (1987). It is available for academic use on a Sun micro computer maintained by the Mechanical Engineering Department at the University of Calgary. ANSYS is capable of linear and non-linear static and dynamic finite element analysis. It is possible to execute the program in either batch mode or interactive mode. Graphical representation of the model and the results is an integral part of the suite. Several pre and post processing programs allow extensive manipulation of the results. The program is very well documented with a user's manual (in two volumes), a theoretical manual, and a manual containing example analyses.

The element library contains approximately 100 elements of all types. A good assortment of material models are also available. The solution procedure is based on a stepwise iterative approach, with or without recalculation of the stiffness matrix after each iteration, as the user sees fit. A frontal solution technique has been implemented into the program.

4.2.1 Concrete Element Formulation

ANSYS allows the non-linear concrete material model to be used only with one element type, an eight node isoparametric brick element. The element is based on a standard isoparametric formulation with an option to include additional shape functions associated with mid-side nodes as described by Wilson (1973). The element has the following capabilities, limits and assumptions:

- Gaussian integration of order 2x2x2 is used to numerically integrate the element.
- Cracking and crushing are allowed in three orthogonal directions at each gauss point.
- Reinforcement may be smeared throughout the element in up to 3 independent directions.
- The concrete may undergo plasticity in addition to cracking and crushing.
- Due to the combined non-linearities, load must be applied in very small increments.
- The three dimensional concrete failure surface model is that of William and Warnke (1975).

4.3 Model Details

The model adopted for study is a concrete slab 3 m wide, 3 m long, and 0.25 m deep as illustrated in Figure 4.1. A 6.25 mm steel plate is bonded to the top and bottom surfaces of the slab which is supported vertically along three lines of support at the bottom surface. The slab is comprised of 8 node isoparametric brick elements to model the concrete, and 4 node isoparametric in-plane elements modeling the steel plate top and bottom. Symmetry is used to advantage so that only a quarter section is actually input into the computer. A simulated point load is applied at the centre line of the middle span by applying a concentrated force at four nodes.

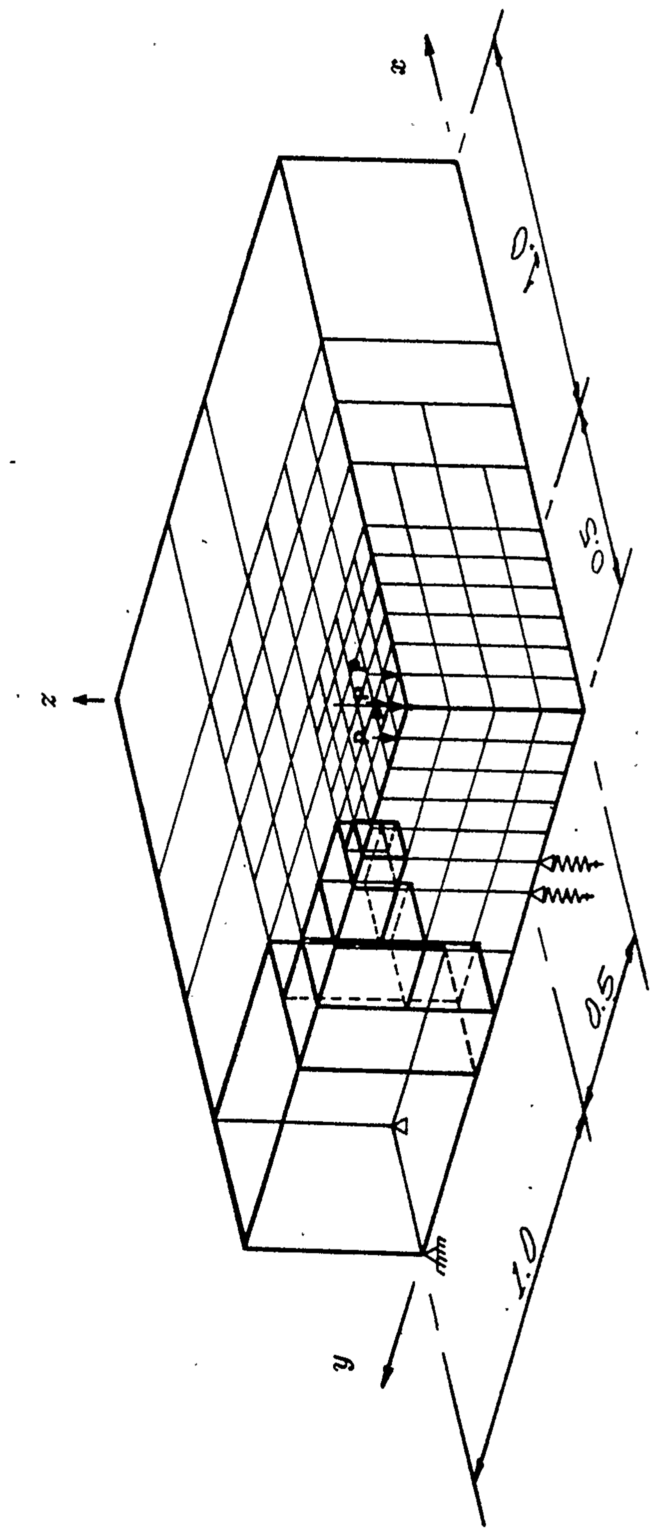

Figure 4.1: Three Dimensional Finite Element Model

Closer examination of Figure 4.1 reveals that the mesh is fine in the vicinity of the load application point, and is progressively expanded to become coarser as it extends outward from the load. In all, six different element types are used to build the model. In the immediate vicinity of the load the model has a block of 144 non-linear concrete elements arranged in a 6x6 grid with 4 elements through the depth. Above and below this block of non-linear concrete elements there are 36 four node linear isoparametric in-plane elements to model the 6.25 mm steel plate.

The remainder of the model is comprised of linear elastic solid and plate elements as required to properly model the steel and concrete. The 8 node isoparametric element used allows the inclusion of any arbitrary number of mid-side nodes, for a maximum of 20 possible nodes. In this model, it is necessary to add two mid-side nodes to some elements. This is because as the mesh progresses outward from the load application point, the elements become larger, and the mesh coarser. In order to allow all nodes to be connected properly to all surronding elements, two additional mid-side nodes are required in addition to the eight corner nodes.

The steel plates on the top and bottom surfaces are modelled with four node isoparametric plate elements. Again, this element allows inclusion of any number of mid-side nodes as required for proper mesh formulation. Therefore, where required, some of the plate elements have one additional mid-side node to connect properly to the surrounding elements.

Vertical support is provided on the bottom surface along the line y = 1.5 m, ie. the outside edge, by restraining the z degree of freedom. The nodes on the bottom surface at y = 0.5 m and y = 0.417 m are supported vertically by attaching stiff grounded springs oriented in the z direction. All in all there are 369 elements and

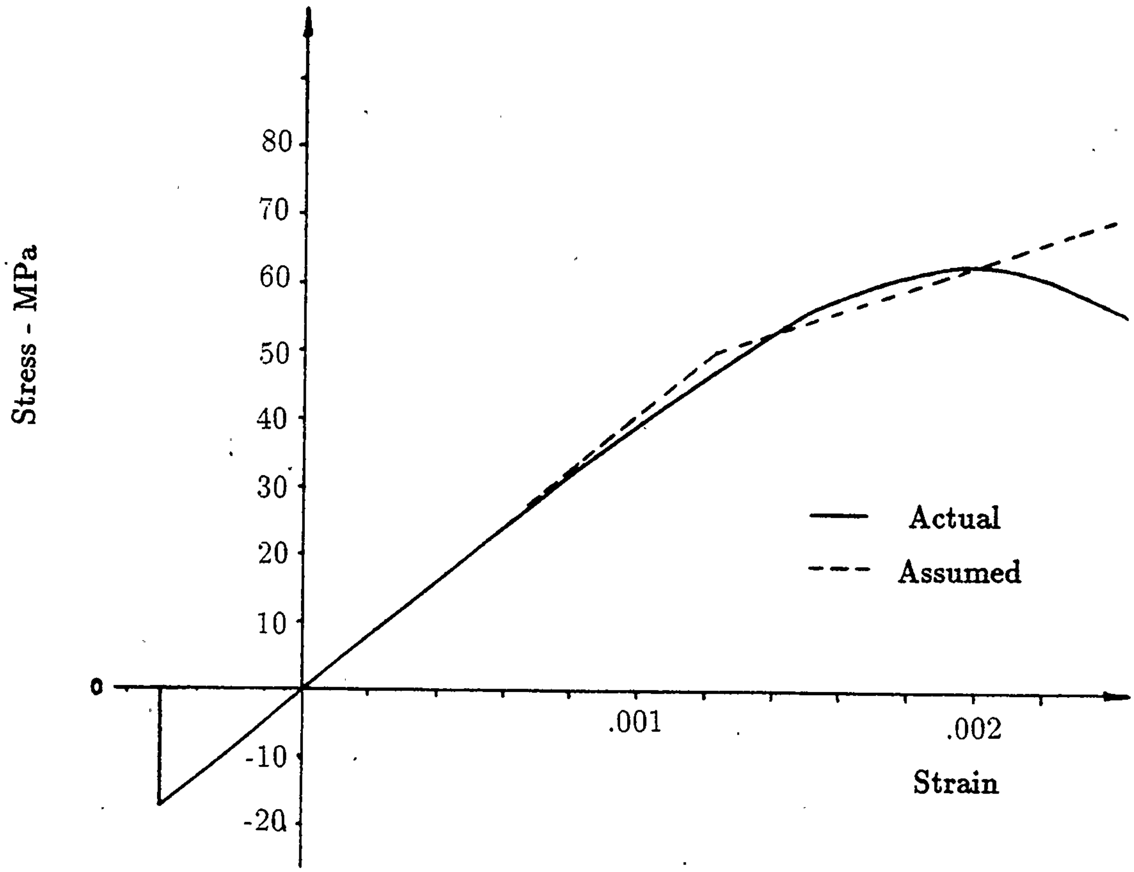

Figure 4.2: Concrete Stress Strain Curve

393 nodes in the model.

The material properties for all the steel elements are the same, with Young's modulus of 200,000 MPa and Poisson's ratio of 0.3. For the linear concrete elements Young's modulus is 40,000 MPa and Poisson's ratio is 0.15. For the non-linear concrete elements a simplified stress-strain curve was adopted as shown in Figure 4.2.

Although the program allows the compression side of the stress-strain curve to be defined with up to five linear line segments, only two were used. There are two reasons for this. The first is that, in the early stages of loading, the main contributing factor to non-linear behaviour is cracking, rather than the non-linear compression. The second reason is that using two linear line segments rather than five increased the speed of execution by a factor of approximately three.

On the tension side, the material model does not allow tension stiffening. As soon as the cracking strain of the material is exceeded, the stress drops to zero. This behaviour, combined with plasticity, leads to a very unstable solution procedure. Results are dependent upon the load path and step size used in the analysis.

4.4 Results of the Three Dimensional Model

The model as described in the previous section was run for a load level of 0.6 MN with both a linear analysis and a non-linear analysis. Deflections, cracks, and steel and concrete stresses are compared for the two cases. First cracks appeared at a load level of 0.4 MN, therefore 0.6 MN is well into the non-linear range. However, this load is much less than the anticipated ultimate collapse load. All attempts to load the non-linear model beyond a load level of 0.6 MN met with failure caused by numerical instability. The exact cause of the problem is not known but it is possibly related to the lack of tension stiffening in the material model. All of the results to be discussed in this section relate to a load level of 0.6 MN.

Figure 4.3 shows the deflected shape along the y-z and the x-z plane for both the linear and non-linear case. Deflections are enlarged 200 times in this plot. Maximum deflection in the linear analysis is 0.3 mm and in the non-linear analysis is 0.362 mm. An analytical solution for a single span with two simply supported edges and using thin plate theory, which neglects through thickness shear effects, results in a deflection of 0.405 mm. A similar solution assuming fixed supports results in a deflection of 0.186 mm. The linear finite element model solution of 0.3 mm falls nicely between these two values. The deflection of the corresponding two-dimensional model, ie. the case of a beam of width 0.375 m, the same span and depth, and with 2.6% reinforcing steel both top and bottom, is 0.22 mm for the Arch support condition, 0.29 mm for the Spring 2 support condition, and 0.53 for the Spring 1 support condition. These deflections are tabulated in Table 4.1

While it would appear that the two-dimensional meshes, with the exception of the Spring 1 support condition, are stiffer than the three-dimensional meshes, this is not the case. Because the 0.6 MN load is applied over the entire 0.375 m width of the two-dimensional model, the deflection is constant over this width. However, for the three-dimensional model the load is applied over a width of 0.166 m, and the deflection is the maximum value at the centre line. The average deflection over a width of 0.375 m is slightly less than the maximum deflection, for example the three-dimensional non-linear FEM has an average deflection of 0.27 mm over this width. This is less than the deflection of the two-dimensional model with the spring 2 support condition, but is greater than the Arch support condition. The best comparison possible is between the two-dimensional three span model and the three-dimensional model, because, aside from the addition of three-dimensional effects, these models are very similar. The effect of the third dimension is to make the three-dimensional slab stiffer than the corresponding two-dimensional model.

Figure 4.3c provides confirmation of the boundary conditions assumed in the two-dimensional study. There is virtually no horizontal movement at the far end of

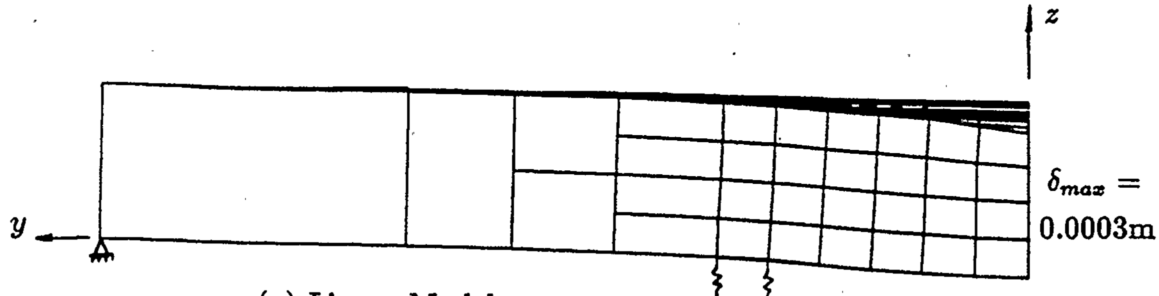

(a) Linear Model - x = 0

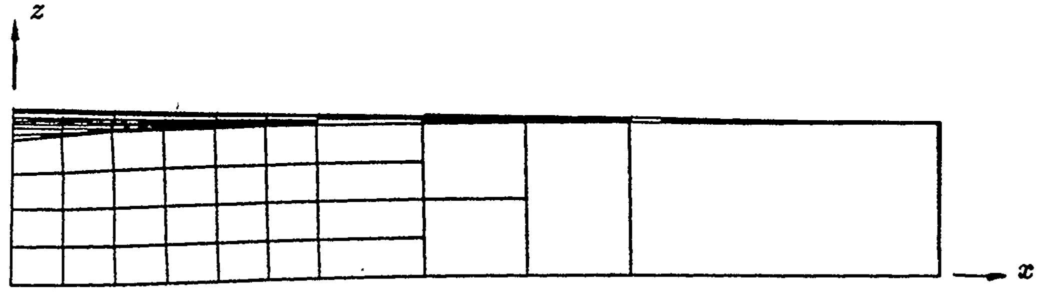

(b) Linear Model - y = 0

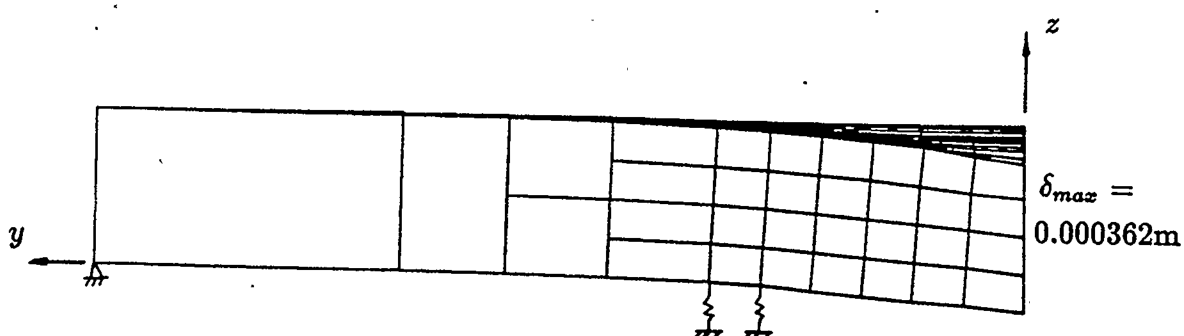

(c) Non-Linear Model - x = 0

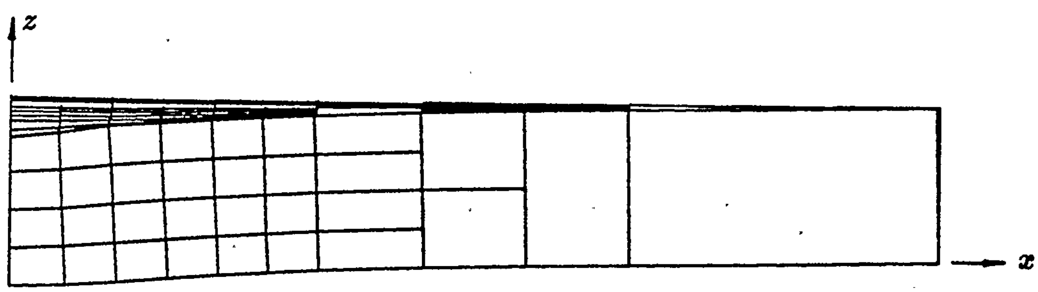

(d) Non-Linear Model - y = 0

Figure 4.3: Deflected Shape Distorted 200 Times

Case	Deflection - mm
Simply supported - Thin Plate Theory	0.405
Fixed Edges -Thin Plate Theory	0.186
3D Linear FEM	0.3
3D Non-Linear FEM	0.362
2D Arch Support FEM	0.22
2D Spring 1 Support FEM	0.53
2D Spring 2 Support FEM	0.29
2D Three Span FEM	0.33

Table 4.1: Deflection for 0.6 MN Load Level

the span adjacent to the loaded span. This means that the assumption of horizontal restraint of this boundary made with the Spring 1, Spring 2, and the Three Span support conditions in the two-dimensional analysis is a fair one.

Stresses in the steel layers are plotted in Figures 4.4 to 4.7. Figure 4.4 shows the σ_x and σy stress along the line x = 0 for both the linear and non-linear analyses. It is seen that, in the immediate vicinity of the load, the steel stresses for the non-linear analysis are significantly higher than the linear analysis. This is as expected because as the concrete cracks in tension in the non-linear analysis, the load is shed to the bottom steel layer.

Similarly, Figure 4.5 shows σx and σy stress along the line y = 0 for both linear and non-linear analyses. The plot of σx exhibits similar behaviour to the σx and σy plots along the x = 0 line. That is, it shows a significant increase in tensile stress of the non-linear analysis in the immediate vicinity of the applied load, but the difference gradually diminishes until the stresses from the two analyses is almost identical. However, the σy stresses remain quite far apart along the line x = 0. This is due to the presence of tensile cracks in the concrete extending along this boundary.

Figure 4.6 shows σx and σy stresses plotted as isobars in the top and bottom

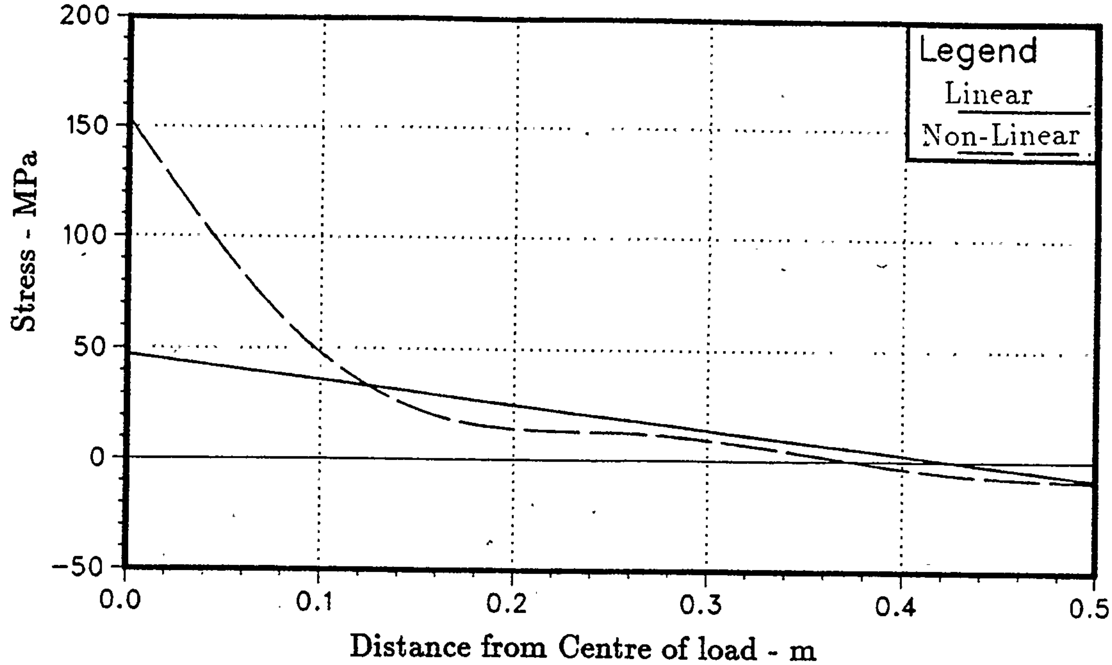

(a) σ_x at $x = 0$

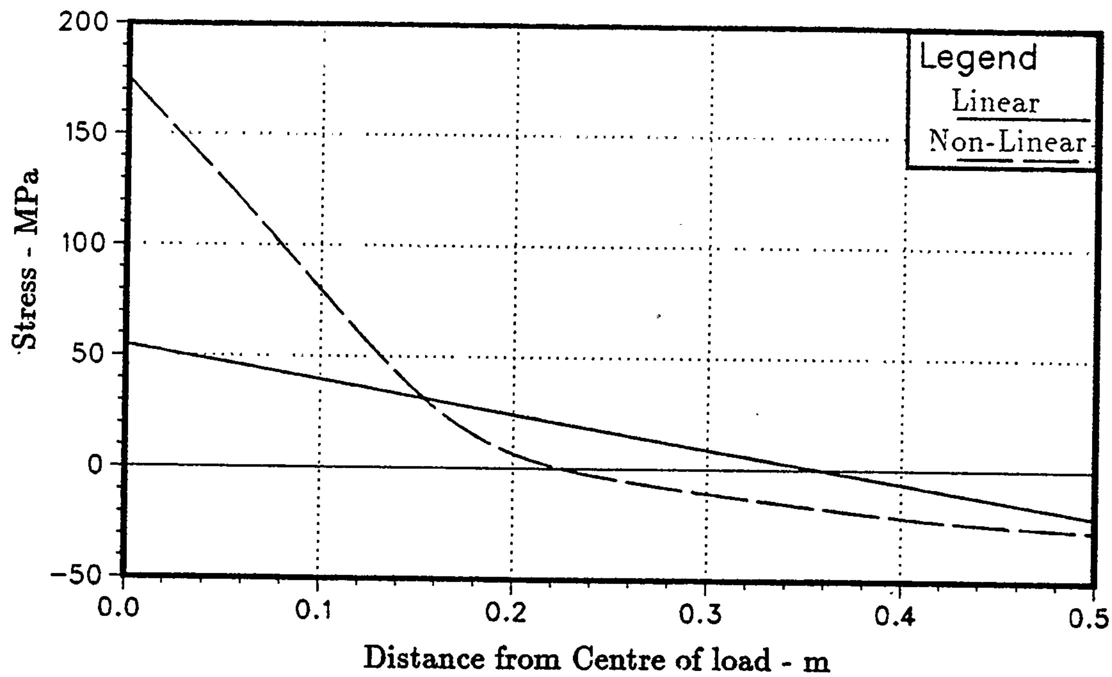

(b) σ_y at $x = 0$

Figure 4.4: Comparison of Bottom Steel Stresses Along the Line X = 0

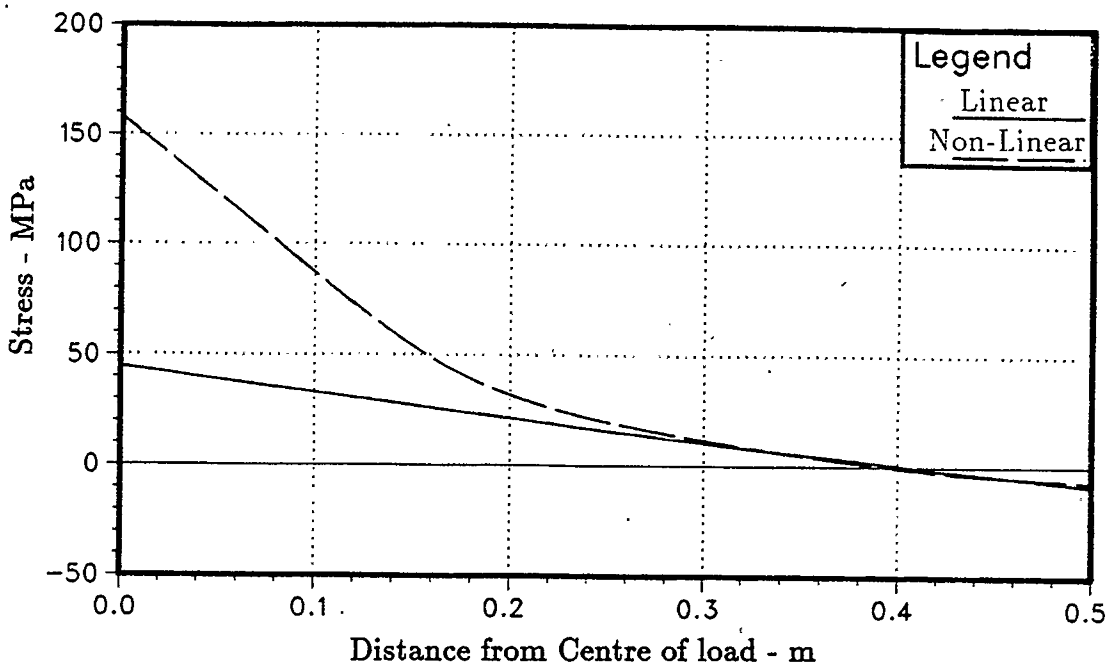

(a) σx at $y = 0$

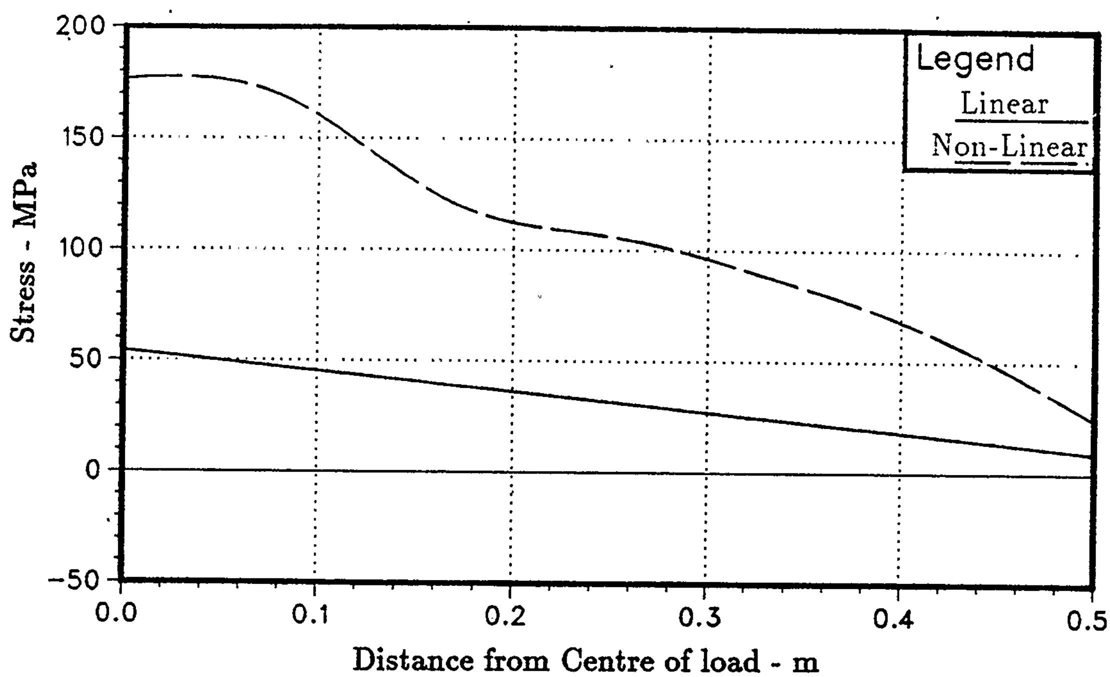

(b) σy at $y = 0$

Figure 4.5: Comparison of Bottom Steel Stresses Along the Line Y = 0

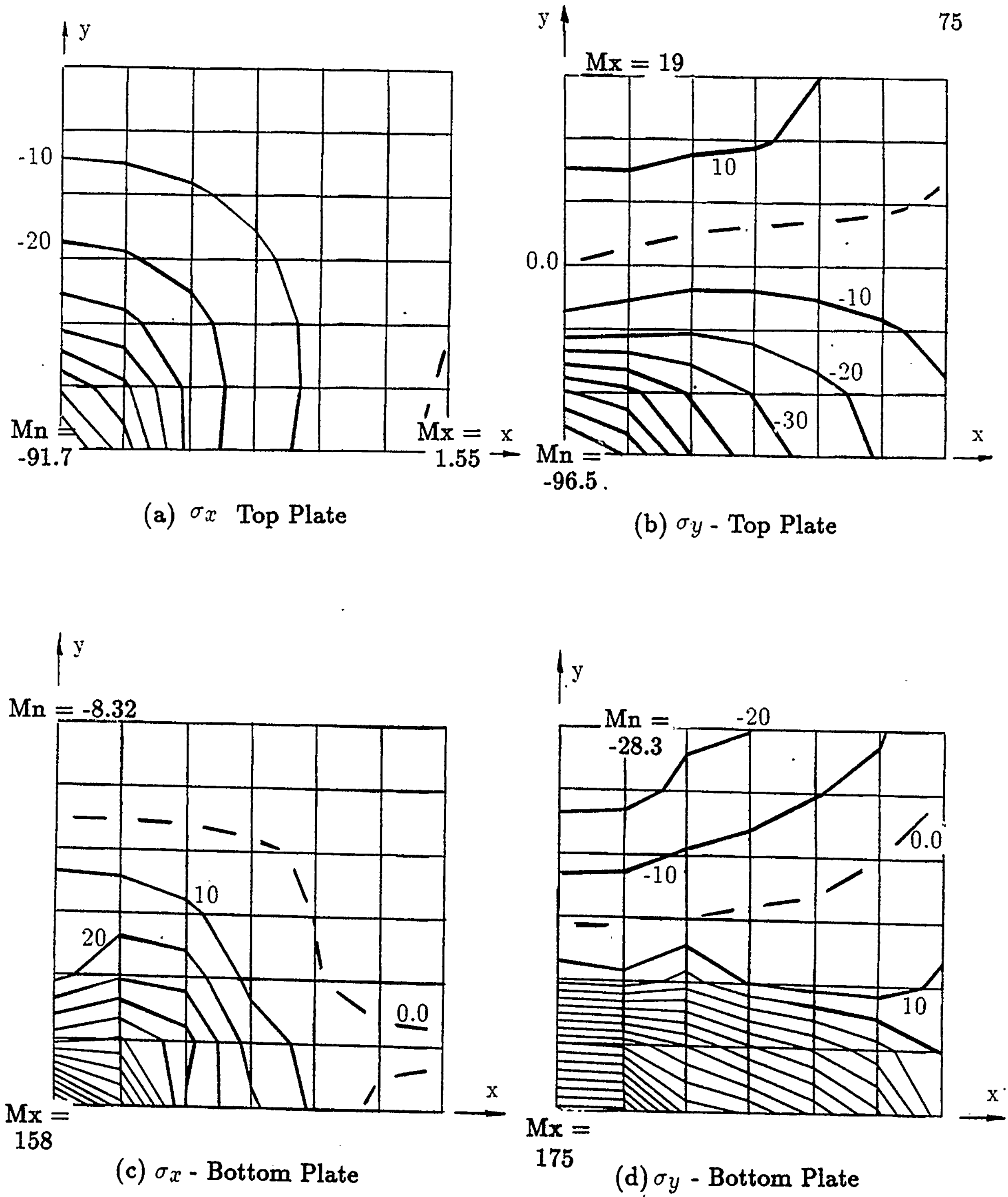

Figure 4.6: Steel Stresses - Non-Linear Model

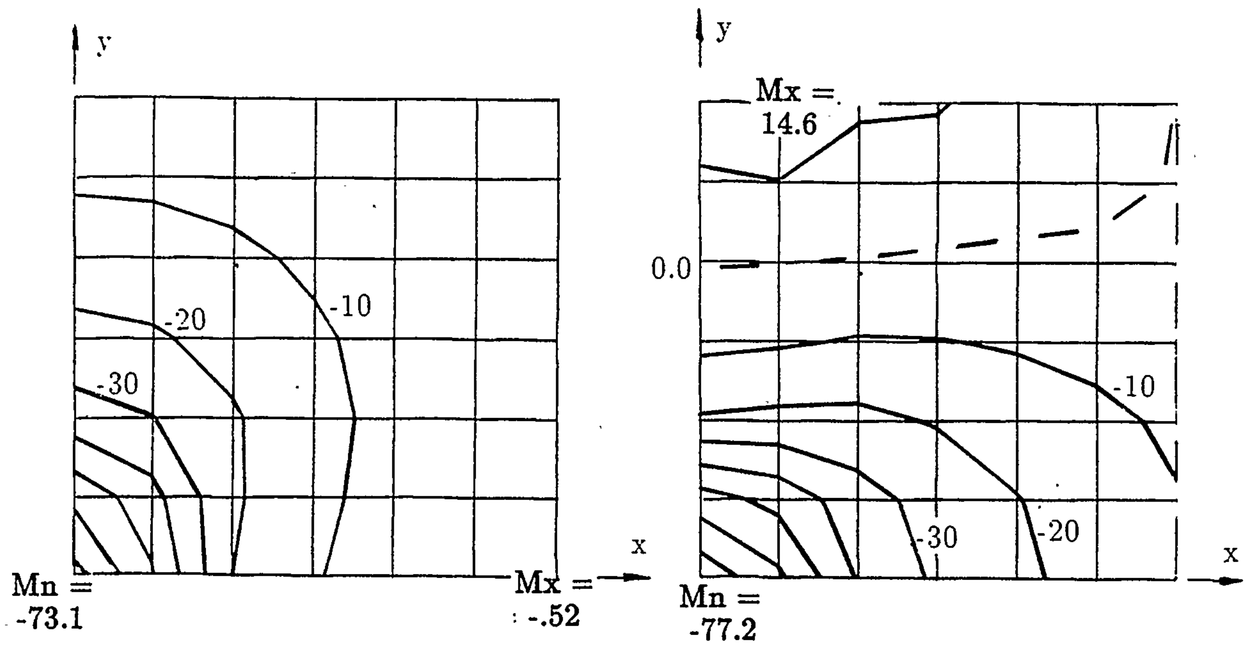

(a) σx - Top Plate

(b) σy - Top Plate

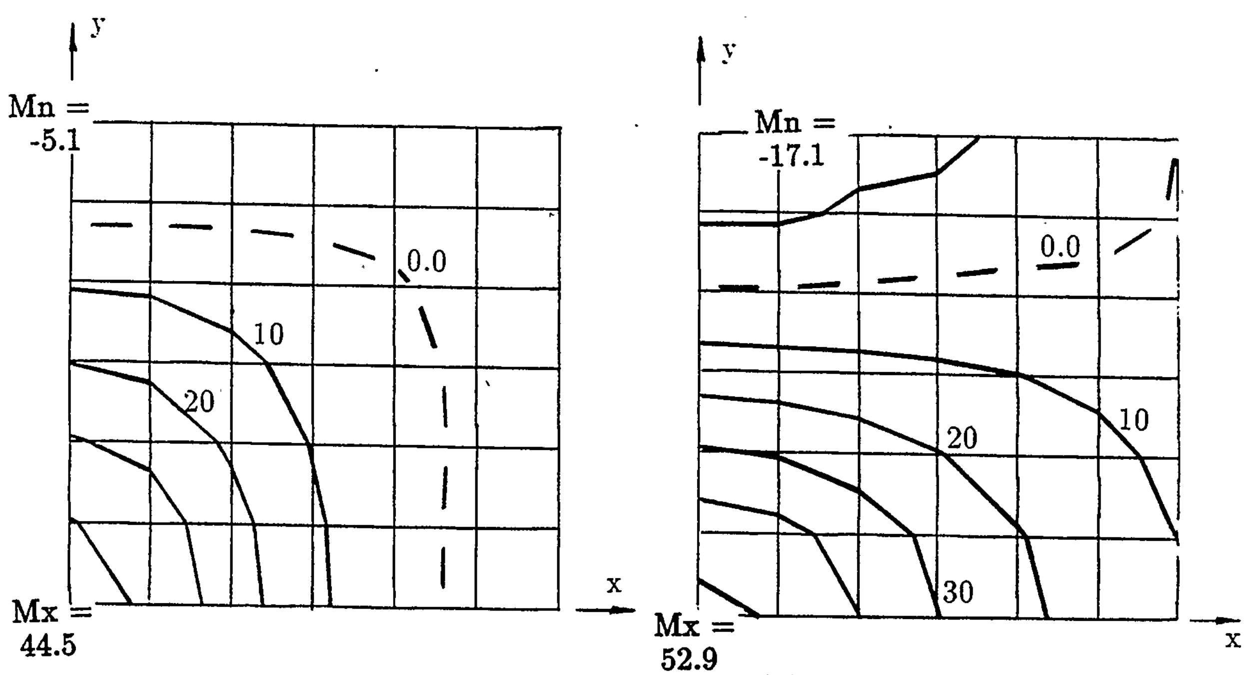

(c) σx - Bottom Plate

(d) σy - Bottom Plate

Figure 4.7: Steel Stresses - Linear Model

steel plates for the non-linear model. Only the steel plate directly above and below the 6x6x4 block of non-linear concrete elements are shown. The load is applied in the lower left hand corner, and the positive x and y global axes are indicated. Isobars are spaced at 10 MPa intervals. A dashed isobar indicates the zero stress level. In addition, the location and magnitude of the maximum (labeled Mx) and minimum (labeled Mn) stress are indicated (tension positive). The location of the elements are indicated by the solid grid of thinner lines. Figure 4.7 shows a similar set of plots for the linear analysis. It can be seen that the stresses in the top plate are almost identical for both the linear and non-linear analyses. The only difference is that the non-linear analysis shows an increase in the compressive stress in the steel plate of about 20 MPa directly under the loaded area. The trends discussed previously for the stress in the bottom plate can be clearly seen here as well.

Generally the differences in steel stresses for the two cases are entirely explained by examining the orientation of the cracks in the concrete elements shown in Figure 4.8. This figure shows a plan view of the cracks in each concrete layer, starting with the bottom layer and progressing upward to the top layer. Again, as for the two dimensional analysis, the lines only illustrate the crack orientation. The length of the lines shown in figure 4.8 has no significance. Recall that this is essentially a one way slab with a line of support directly under the elements indicated in the bottom layer, and the slab centre line is located in the x-z plane. This crack pattern is exactly what one would expect. It fully explains the observed steel stresses in the bottom steel plate.

Finally, the principal compression stresses in the concrete for both the linear and non-linear cases are examined. Figure 4.9 shows the principal stress vectors in the

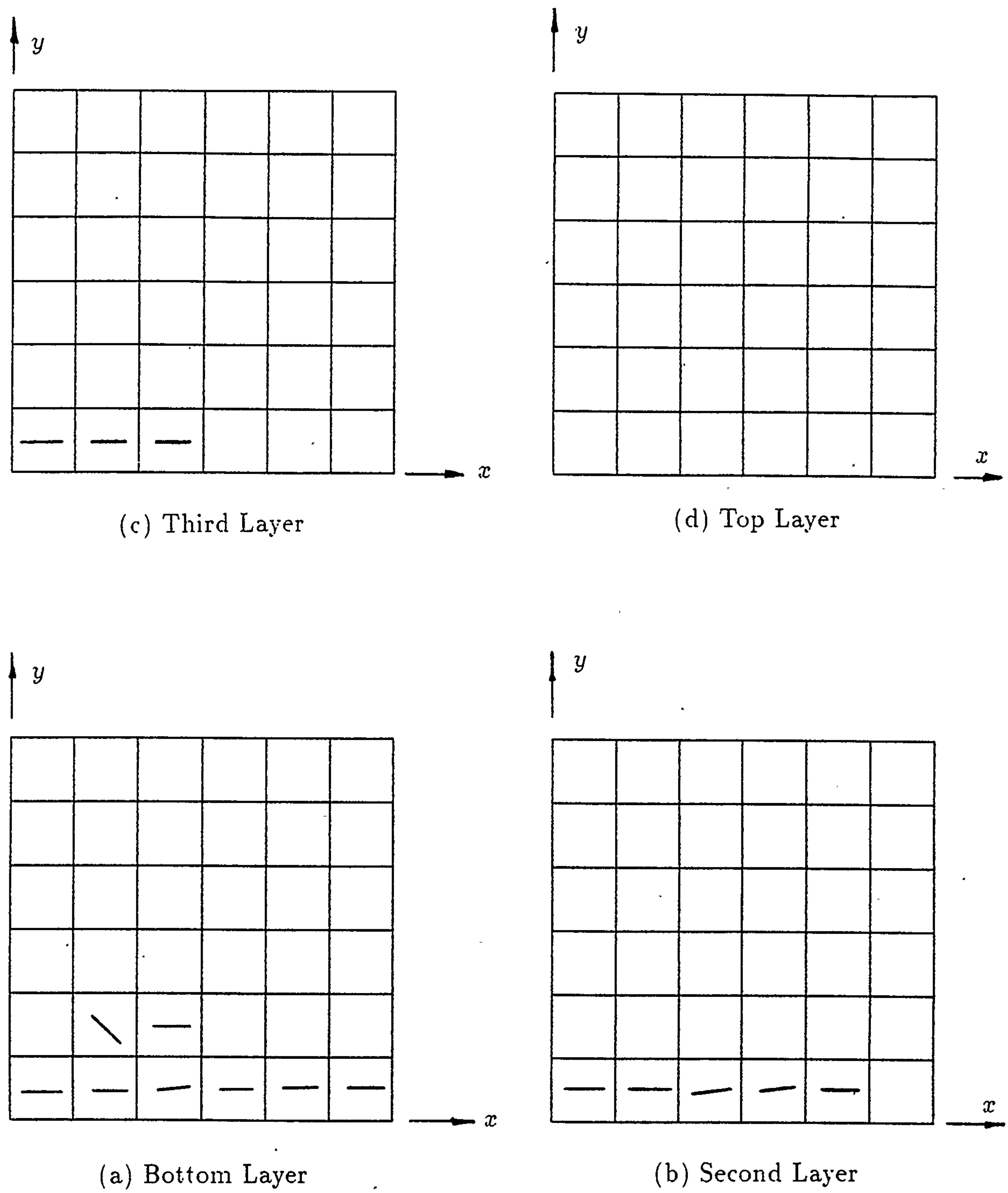

Figure 4.8: Crack Patterns in the Concrete Layers

y-z plane scaled so that 25 MPa is equal to the length of one element. Figure 4.9a shows the results of the linear analysis, and Figure 4.9(b) shows the results of the non-linear analysis. The difference between the two cases is slight. The non-linear case shows a small increase in the magnitude of the compression stresses just over the support, and a slight change in the orientation of the vector directly under the load.

Figure 4.9c shows the principal compression stress vectors for the fully restrained two dimensional model with steel top and bottom at a load level of 0.6 MN. It is substantially different from the pattern of the three dimensional analysis, except in the immediate vicinity of the applied load. The reason for this drastic difference is that, in the two dimensional case, load is transferred directly from the application point to the support. Because the beam is constant width, the concrete failed simultaneously at the load point and just above the support. However, in the three dimensional model, load can be transferred in two directions. Similar to the two dimensional model, the load can flow in the y-z plane, and this certainly occurs as indicated in Figure 4.9. But, load can also flow in the x-y plane as well. By the time the stresses reach the support, they have been distributed so much in the x direction that they are negligible. For this reason there can be no direct comparison of the principal compression stresses of the two dimensional and the three dimensional models.

Figure 4.10 shows the principal compression stresses in the x-z plane for both the linear and non-linear models. The magnitude of the compression stress directly under the load is virtually identical to that of y-z plane, indicating that force does indeed flow in the x-z plane. Again, there is little difference between the linear and non-linear results.

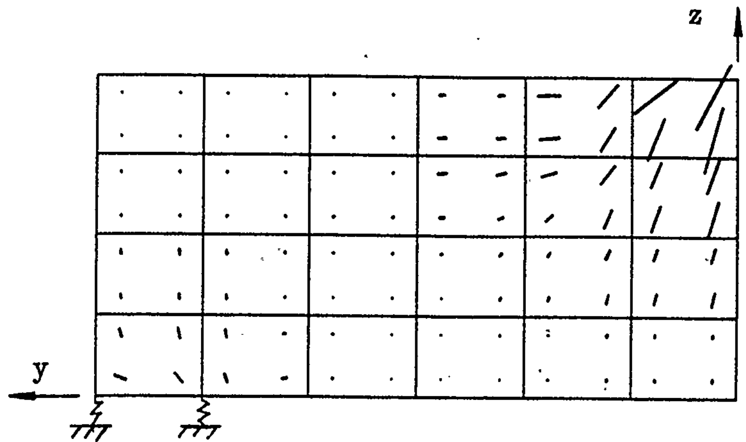

(a) Three Dimensional Linear

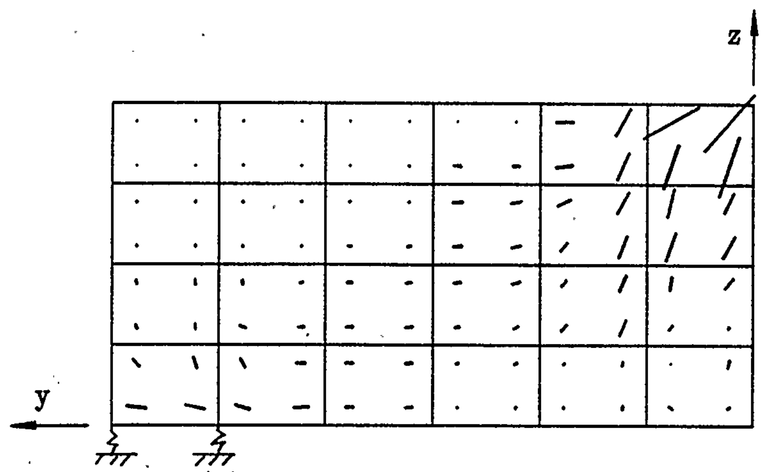

(b) Three Dimensional Non - Linear

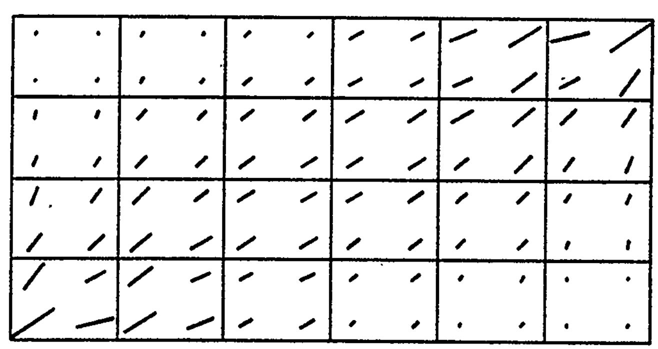

(c) Two Dimensional Non - Linear

Figure 4.9: Principal Compression Stress Vectors in the Y - Z Plane

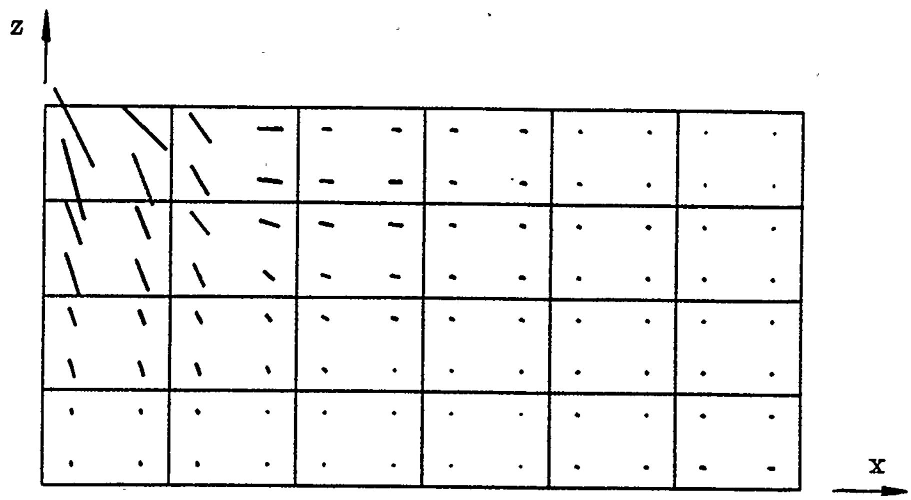

(a) Linear

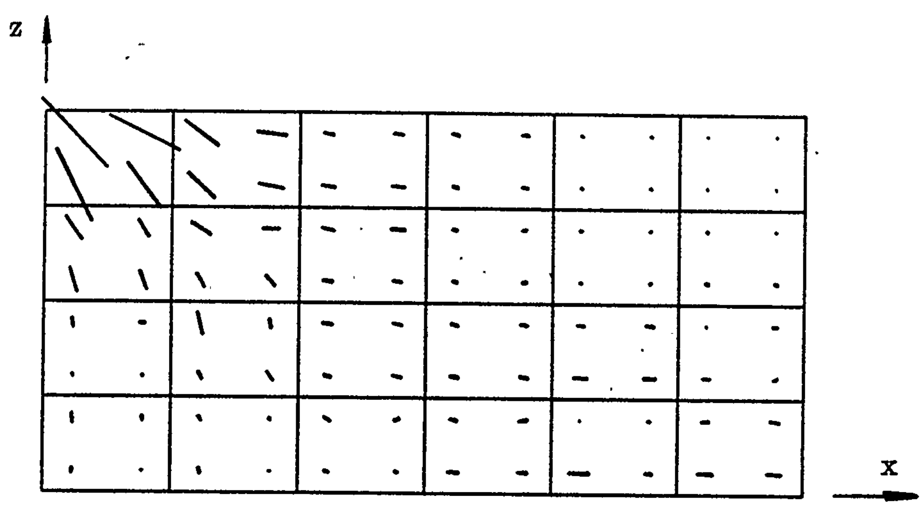

(b) Non - Linear

Figure 4.10: Principal Compression Stress Vectors in the X - Z Plane

Chapter 5

Conclusions and Recommendations

5.1 Conclusions

The following conclusions are drawn from the work presented herein. It is hoped that these conclusions will assist, at least in some small way, in understanding the analysis of compressive membrane action in deep beams and slabs.

The problems and difficulties encountered during both the two dimensional and the three dimensional analysis lead one to conclude that non-linear finite element analysis is an impractical tool to use in design, except in very special cases. The simplified strut model provides a remarkably good tool for the evaluation of compressive membrane action in deep beams with rigidly restrained boundary conditions and no reinforcing steel. If the boundary is not perfectly rigid, or a small amount of reinforcing steel added, the model will become less accurate. However, with further work it would likely prove to be an adequate model for design purposes.

FELARC proved to be a very sophisticated and powerful analysis tool for two dimensional problems of this type. The addition of a post-processing routine to plot deformations, stress and crack distributions, and load deflection curves greatly enhanced the usefulness of the program. Because the formulation of the shell element is based on thin plate theory, the program is not suitable for three dimensional problems when through thickness shear effects cannot be ignored.

The following conclusions are applicable for the particular loading and geometry studied herein. Specifically, they apply to concrete beams with concentrated point loads at the centre of the span, or to one-way slabs with a line load or point load at the span centre line. Span to depth ratio is a crucial factor in this type of analysis, therefore the conclusions are limited to beams and slabs with a relatively small span to depth ratio of about four to eight.

The factors studied in the two dimensional parametric study are span to depth ratio, the lateral stiffness of the boundary, the amount and arrangement of longitudinal reinforcement, and the type of shear connection provided between the concrete and steel. These factors will be discussed in greater detail.

The most important factor in the development of CMA in deep beams and slabs is the span to depth ratio. For a given length of beam, an increase in the depth of the cross section will provide a proportional increase in the load carried by the member in CMA. Alternatively, for a given depth of beam, a decrease in the length of the beam will result in an increase in the load carried by CMA. As shown in the two-dimensional parametric study, this is true regardless of the amount or arrangement of longitudinal steel. Furthermore, the analytical strut model developed indicates the same relationship between span to depth ratio and load capacity. Because of simplifications made in the development of the strut theory, the deflections predicted by the strut theory are larger than those predicted by both the two and three dimensional finite element models.

It is also obvious that the concrete strength in compression is just as important as span to depth ratio. An increase in the nominal compressive strength of the concrete will also provide a proportional increase in the load carried by the member in CMA.

The second most important factor in the development of CMA is the amount of in-plane restraint at the boundary of the member. Varying the boundary condition from fully restrained, to one partially restrained by the Spring 1 support condition resulted in a reduction of the load carrying capacity of about 30%, regardless of the amount or arrangement of longitudinal reinforcing steel. This indicates that the load carried by CMA is sensitive to the actual boundary conditions. However, a number of factors not studied in this work could also have an influence on the sensitivity of the ultimate load carrying capacity to the support conditions. These include the actual loading conditions, the vertical stiffness of the support, and the span to depth ratio.

The third most important factor in the development of compressive membrane action is the arrangement of longitudinal reinforcing steel. The addition of 2.6% reinforcing steel both top and bottom increased the load carrying capacity by approximately 20%, regardless of the support condition. This is not as suprising as it might first seem. The horizontal thrust provided by the support itself essentially takes the place of longitudinal reinforcing steel, making the steel redundant. The capacity of the member is governed by the compressive strength of the concrete, resulting in very little change in the ultimate load carrying capacity when longitudinal steel is added.

Finally, the factor with the least significance is the type of shear connection. The addition of diaphragms connecting the top and bottom plates provided only a moderate increase in load carrying capacity of 5% to 10%, regardless of the support condition. Short shear studs, as represented by the beam shown in figure 3.14c, long shear studs and diaphragms all provided approximately the same ultimate load carrying capacity. Serviceability and ease of fabrication will be the two most important factors in the selection of a shear connection scheme. It should be noted that the effect of no shear connection at all was not considered in the study. In any case, it would be impractical to fabricate such a member because the steel plate in the compression zone would separate from the concrete and buckle at a relatively low load.

The use of a two dimensional study is adequate for determining the behaviour of beams, and for slabs which can be analyzed using beam strips, such as a slab with a line load. However, the use of a two dimensional model to simulate a three dimensional situation is of marginal use because the load carrying mechanisms are sufficiently different as to render any comparison questionable. The primary cause of failure in the two dimensional case is generally bi-axial compression causing crushing of the concrete simultaneously at the two nodes, ie. directly under the load and directly over the support. In a three dimensional slab subjected to a point load, crushing would not occur over the support, but would take place directly under the load. Because the concrete in this location is in a tri-axial state of stress, both its strength and ductility will be greater than the corresponding two dimensional case. The apparent ultimate load carried by CMA in three dimensional slabs will depend highly on the actual behaviour of the concrete in a state of tri-axaial compression. However, because the load carrying mechanisms are of the same type, it is expected that the relative importance of the factors considered in the two dimensional study would be the same in the three dimensional case.

When testing physical specimens or performing numerical analysis of deep beams and slabs, the utmost attention must be paid to the proper modelling of the support conditions and load application details. In particular, improper modelling of in-plane restraint at the boundary could cause a serious underestimation of the ultimate load carrying capacity and ductility of such members.

When designing deep, continuous beams and slabs, a substantial cost saving could result from the consideration of the beneficial effects of compressive membrane action. In particular, the effective reinforcement ratio could be drastically reduced with no sacrifice in either ultimate strength or serviceability requirements.

5.2 Recommendations for Future Research

A very few recommendations for further work in this area are presented with the hope that an ambitious gradute student will pursue at least one of them.

In order to verify the results of the numerical simulation, it is necessary to conduct physical testing in the laboratory. In order to do this, a test frame is required with which the stiffness of the in-plane restraint and the amount of in-plane force can be measured and adjusted. Such a test frame is being built by the Centre for Frontier Engineering Research (CFER) at the University of Alberta in Edmonton, and should be ready for use in the near future.

The commercially available finite element packages investigated during the course of this study all had major flaws or inherent limitations which rendered them of marginal use in this study. However, in spite of the difficulties associated with non-linear finite element modelling of reinforced concrete, the possible benefits of a well designed and tested three dimensional finite element program are great. In particular, the development of such a program should be done with consideration of the following:

- A very stable solution technique and a concrete material model including tension stiffening and the capability of modelling the descending part of the compression side of the stress-strain curve, such as implemented in FELARC, should be included. Also, an interface element for modelling bond slip between steel and concrete should be included.

- As difficult as it is to obtain results in three dimensional finite element modelling of reinforced concrete, it is many more times difficult to interpret them. A well structured, versatile, and easy to use post processing program for the printing and plotting of results is a necessary feature of such a program. This cannot be emphasized enough. Properly analyzing the results from a large three dimensional model would be a hopelessly futile endeavor without the aid of a well designed post-processing program.

- The availability of the worlds most powerful vector computer at the University of Calgary should be exploited. With the Cyber 205 Supercomputer, and a properly designed and written program, it would be possible to conduct numerical simulations of large, non-linear, three dimensional problems that are not currently feasible on any other computer. Because the architecture of the vector computer is different from that of a scalar computer, in general it is not possible to transfer existing programs from a scalar computer to a vector computer and obtain optimum performance. Usually, to obtain satisfactory utilization of the power of the vector processor, it is necessary to design and write a program specifically for the vector computer available, in this case a Cyber 205 Supercomputer.

Bibliography

[1] Adams, P. F., Zimmerman, T. J. E. and MacGregor, J. G., 1987. *Design and Behaviour of Composite Ice Resisting Walls.* POAC'87. The 9th International Conference on Port and Ocean Engineering Under Arctic Conditions, Fairbanks, Alaska, August, 1987.

[2] Braestrup, M. W., 1980. *Dome Effects in RC Slabs: Rigid-Plastic Analysis.* Journal of the Structural Division, Proceedings of the American Society of Civil Engineers, Vol 106, No. ST6, June, 1980. pp. 1237-1253.

[3] Brotchie, J. F. and Holley, M. J., 1971. *Membrane Action in Slabs.* ACI Publication SP-30, Cracking, Deflection, and Ultimate Load of Concrete Slab Systems. 1971. pp. 345-377.

[4] Cope, R. J. and Clark, L. A., 1984. *Concrete Slabs Analysis and Design.* Elsevier Applied Science Publishers, London and New York. 1984.

[5] Ghoneim, G. A. M. and Ghali, A., 1979. *User Manual for Computer Program FELARC.* Department of Civil Engineering Research Report No. CE78-15, University of Calgary, 1979.

[6] Ghoneim, G. A. M., 1978. *Nonlinear analysis of Concrete Structures.* Ph.D. Thesis, Department of Civil Engineering, University of Calgary, August, 1978.

[7] Hewitt, B. E. and Batchelor, B., 1975. *Punching Shear Strength of Restrained Slabs.* Journal of the Structural Division, Proceedings of the American Society of Civil Engineers, Vol 101, No. ST6, September, 1975. pp. 1837-1853.

[8] Hopkins, D. C. and Park, R., 1971. *Test on a Reinforced Concrete Slab and Beam Floor Designed with Allowance for Membrane Action.* ACI Publication SP-30, Cracking, Deflection, and Ultimate Load of Concrete Slab Systems. 1971. pp. 223-250.

[9] Kinnunen, S. and Nylander, H., 1960. *Punching of Concrete Slabs Without Shear Reinforcement.* Transactions of the Royal Institute of Technology, Stockholm, Sweden, no. 158, 1960.

[10] Kirkpatrick, J., Rankin, G. I. B. and Long, A. E., 1984. *Strength Evaluation of M-Beam Bridge Deck Slabs.* The Structural Engineer, Vol 62B, No. 3, September, 1984. pp. 60-68.

[11] Kirkpatrick, J., Rankin, G. I. B. and Long, A. E., 1986. *The Influence of Compressive Membrane action on the Serviceability of Beam and Slab Bridge Decks.* The Structural Engineer, Vol 64B, No. 1, March, 1986. pp. 7-9.

[12] Maddock, W. J., and Bruce, J. C., 1984. *The Potential for Combining Structural Steel and Concrete in Arctic Structures.* Icetech 84, The Third Symposium on Marine Problems in Ice-Infested Waters. SNAME, The Society of Naval Architects and Marine Engineers, Arctic Section, Calgary, Alberta, May, 1984.

[13] Matsuishi, M., Nishimaki, K., Takeshita, H., Iwata, S. and Suhara, T., 1977. *On the Strength of Composite Steel Concrete Structure of a Sandwich System (1st Report) - Experiment of Statical Strength and Ultimate Strength Analysis.* Hitachi Zosen Technical Review, Vol 38, Osaka. September, 1977.

[14] Matsuishi, M., Nishimaki, K., Iwata, S. and Suhara, T., 1978. *On the Strength of Composite Steel Concrete Structure of a Sandwich System (2nd Report) - Non-Linear Analysis using Finite Element Analysis.* Hitachi Zosen Technical Review, Vol 39, Osaka. March, 1978.

[15] Matsuishi , M., Nishimaki, K., Iwata, S. and Suhara, T., 1980. *On the Strength of Composite Steel Concrete Structure of a Sandwich System (3rd Report) - Effect of Repeated Loadings.* Hitachi Zosen Technical Review, Vol 40, Osaka. March, 1980.

[16] Matsuishi, M., Nishimaki, K., Iwata, S. and Suhara, T., 1980. *On the Strength of Composite Steel Concrete Structure of a Sandwich System (4th Report) - Effect of Girder Web.* Hitachi Zosen Technical Review, Vol 41, Osaka. December, 1980.

[17] Matsuishi, M., and Iwata, S., 1987. *Strength of Composite Sandwich System Ice Resisting Structures.* POAC'87. The 9th International Conference on Port and Ocean Engineering Under Arctic Conditions, Fairbanks, Alaska, August, 1987.

[18] Nielsen and Braestrup, M. W., 1978. *Shear Strength of Prestressed Concrete Beams Without Web Reinforcement.* Magazine of Concrete Research, Vol 30, No 104, September, 1978.

[19] O'Flynn, B., and MacGregor, J. G., 1987. *Tests on Composite Ice Resisting Walls.* POAC'87. The 9th International Conference on Port and Ocean Engineering Under Arctic Conditions, Fairbanks, Alaska, August, 1987.

[20] Ontario Ministry of Transportation and Communications, 1979. *Ontario Highway Bridge Design Code 1979.*

[21] Saenz, L. P., 1964. *Discussion of Equation for the Stress-Strain Curve of Concrete.* by Desayi and Krishnan, ACI Journal, Proc. Vol 61, No. 9, September, 1964, pp. 1229-1235.

[22] Smith, G. M. and Young, L. E., 1955. *Ultimate Theory in Flexure by Exponential Function.* Journal of the ACI, Vol 52, No. 3, November 1955, pp. 349-359.

[23] Smith, J. R. and McLeish, A., 1987. *The Resistance of Composite Steel/Concrete Structures to Localized Ice Loading.* POAC'87. The 9th International Conference on Port and Ocean Engineering Under Arctic Conditions, Fairbanks, Alaska, August, 1987.

[24] Taylor, F. W. Thompson, G. E., and Smulski, E., 1925. *Concrete, Plain and Reinforced.* Vol 1, 4th edition, John Wiley and Sons, New York, 1925.

[25] Tong, P. Y. and Batchelor, B., 1971. *Compressive Membrane Enhancement in Two-Way Bridge Slabs.* ACI Publication SP-30, Cracking, Deflection, and Ultimate Load of Concrete Slab Systems. 1971. pp. 271-287.

[26] Westergaard, H. M. and Slater, W. A., 1921. *Moments and Stresses in Slabs.* Proceedings of the American Concrete Institute, Vol 17, 1921. pp. 415-538.

[27] Zsutty, T., 1968. *Beam Shear Strength Prediction by Analysis of Existing Data.* American Concrete Institute Journal, Vol 65, November, 1968.